Mandible and teeth characterization of the Gravettian child from Gargas, France

Mona Le luyer, Sébastien Villotte, Priscilla Bayle, Selim Natahi, Adrien Thibeault, Bruno Dutailly, Carole Vercoutère, Catherine Ferrier, Christina San Juan-Foucher, Pascal Foucher

BMSAP

Bulletins et mémoires de la Société d'Anthropologie de Paris
BMSAP

34 (1) | 2022
Entre vivants et morts : regards croisés sur une frontière relative et fluctuante

Mandible and teeth characterization of the Gravettian child from Gargas, France

Caractérisation de la mandibule et des dents de l'enfant gravettien de Gargas, France

Mona Le Luyer, Sébastien Villotte, Priscilla Bayle, Selim Natahi, Adrien Thibeault, Bruno Dutailly, Carole Vercoutère, Catherine Ferrier, Christina San Juan-Foucher and Pascal Foucher

OpenEdition Journals

Electronic version
URL: https://journals.openedition.org/bmsap/9810
DOI: 10.4000/bmsap.9810
ISSN: 1777-5469

Publisher
Société d'Anthropologie de Paris

Electronic reference
Mona Le Luyer, Sébastien Villotte, Priscilla Bayle, Selim Natahi, Adrien Thibeault, Bruno Dutailly, Carole Vercoutère, Catherine Ferrier, Christina San Juan-Foucher and Pascal Foucher, "Mandible and teeth characterization of the Gravettian child from Gargas, France", *Bulletins et mémoires de la Société d'Anthropologie de Paris* [Online], 34 (1) | 2022, Online since 23 March 2022, connection on 27 March 2022. URL: http://journals.openedition.org/bmsap/9810 ; DOI: https://doi.org/10.4000/bmsap.9810

Mandible and teeth characterization of the Gravettian child from Gargas, France

Caractérisation de la mandibule et des dents de l'enfant gravettien de Gargas, France

Mona Le Luyer [1*], Sébastien Villotte [2,3*], Priscilla Bayle [1], Selim Natahi [1], Adrien Thibeault[1], Bruno Dutailly [1,4], Carole Vercoutère [5], Catherine Ferrier [1], Christina San Juan-Foucher[6,7], Pascal Foucher [6,7]

1 UMR 5199 PACEA, CNRS, Université de Bordeaux, Pessac, France
2 UMR 7206 Eco-anthropologie, MNHN, CNRS, Université Paris Cité, Musée de l'Homme, Paris, France
3 Directorate Earth and History of Life, Royal Belgian Institute of Natural Sciences, Belgique
4 UMS 3657 Archéovision, CNRS, Université Bordeaux-Montaigne, Pessac, France
5 UMR 7194 HNHP, Département Homme et Environnement, CNRS, MNHN, Paris, France
6 SRA Occitanie, Toulouse, France
7 UMR 5608 TRACES, CNRS, Université Toulouse Jean Jaurès, Toulouse, France

* mona.leluyer@outlook.com / sebastien.villotte@cnrs.fr

Reçu : 23 juin 2021 ; accepté : 3 novembre 2021
Bulletins et Mémoires de la Société d'Anthropologie de Paris

Abstract – While affinities and interactions between archaic and modern human populations (i.e. 200,000-40,000 BP in Eurasia) at macro-evolutionary and continental scales have received considerable attention, there has been less emphasis on the population history of Europe between 40,000 and 26,000 BP (i.e. prior to the Last glacial Maximum, LGM) when only modern humans were present. Here we examine the immature mandible from Gargas (France, ca. 29,000 cal BP), which displays a modern morphology overall with some archaic features rarely seen, if at all, in European Pleistocene and Holocene modern humans. In particular, the Gargas child has a very broad mandible, large tooth crowns with extreme deciduous and permanent mesiodistal molar diameters and a deciduous first molar with a quantity of enamel never previously reported. Furthermore, this child exhibits a supernumerary permanent tooth in the incisor region, a rare congenital disorder so far described for only five other pre-LGM modern humans. Finally, our results also highlight previously undocumented spatial differences in the tooth crown dimensions of Upper Palaeolithic fossils.

Keywords – mandible, teeth, immature, Gravettian

Résumé – Alors que les affinités et les interactions entre les populations humaines archaïques et modernes sont largement évaluées à des échelles macroévolutives et continentales (i.e. 200 000-40 000 BP en Eurasie), peu d'accent est mis sur l'histoire de la population européenne entre 40 000 et 26 000 BP (i.e. avant le dernier maximum glaciaire, LGM) lorsque seuls les humains modernes étaient présents. Ici, nous examinons la mandibule immature de Gargas (France, *ca.* 29 000 cal BP) qui présente une morphologie globale moderne avec des caractéristiques archaïques rarement ou jamais vues chez les humains modernes du Pléistocène européen et de l'Holocène. En particulier, l'enfant de Gargas présente une très grande largeur mandibulaire, de grandes couronnes dentaires avec des diamètres mésiodistaux extrêmes pour les molaires déciduales et permanentes, et une quantité importante d'émail pour sa première molaire déciduale précédemment inconnue. De plus, cet enfant présente une dent permanente surnuméraire dans la région incisive, un trouble congénital rare décrit pour au moins cinq autres humains modernes pré-LGM. Enfin, nos résultats ont également mis en évidence des différences spatiales auparavant non documentées dans les dimensions des couronnes dentaires des fossiles du Paléolithique supérieur.

Mots clés – mandibule, dents, immature, Gravettien

Introduction

In studies on the population history of Europe during the Upper Palaeolithic (UP, 45,000-10,000 BP), particular emphasis is placed on the initial UP phase (ca. 45,000-40,000 BP) in order to address the following questions: how and when the first anatomically modern human groups arrived in Europe (Benazzi et al., 2011; Higham et al., 2011), the timing of their expansion (Hublin et al., 2020) and the replacement of declining Neandertal populations and their partial absorption by modern humans (Slon et al., 2018; Villanea and Schraiber, 2019). Population dynamics during the UP, when only anatomically modern humans were present on the continent, are comparatively less studied, and little is known about the interactions of European modern human groups from 40,000 BP to the end of the Last Glacial Maximum (LGM, ca. 26,500-20,000 BP).

Western Eurasian pre-LGM modern human remains are relatively abundant, mainly due to the large number of Mid Upper Palaeolithic (MUP, ca. 33,000-24,000 BP) primary burials, most being associated with the Gravettian techno-complex (Henry-Gambier, 2008a). The vast majority of pre-LGM specimens are from adults and adolescents (Henry-Gambier, 2008a; 2008b). Adult skeletons are relatively well documented (Trinkaus, 2007; Holt and Formicola, 2008; Villotte et al., 2017) and characterized by an overall "modern" (derived) human morphology, but "archaic" (plesiomorphic) traits and/or Neandertal features are frequently found in pre-LGM individuals (Trinkaus, 2007). No clear chronogeographical pattern has been detected so far for the distribution of these traits, and the morphology of Early Upper Palaeolithic (EUP, ca. 45,000-33,000 BP) and MUP specimens appears homogenous overall (Mounier et al., 2020), which is consistent with ancient DNA studies that suggested genetic continuity between at least some EUP and MUP individuals (Fu et al., 2016; Posth et al., 2016; Sikora et al., 2017).

Unlike those of adults, well-preserved skeletal remains of pre-LGM children are rare (Zilhão and Trinkaus, 2002) and little is known about their morphology, growth and developmental patterns. One of the best preserved immature skeletons, the 4-5 year-old MUP individual Lagar Velho 1 from Portugal (Zilhão and Trinkaus, 2002), displays a pattern of maturation of its deciduous and permanent dentition and endostructural tooth organization that is absent in extant populations and documented only among Neandertals (Bayle et al., 2010). The immature mandible of El Castillo 2 from Spain (Garralda et al., 2019), belonging to another 4-5 year-old MUP child, shows a modern morphology overall (including its dental maturation pattern) combined with robust characteristics of the symphysis. Other well-preserved immature facial remains with mixed dentition are extremely rare (e.g. Sunghir 3, Kostënki 3 and 4) in the pre-LGM European fossil record (Trinkaus et al., 2014) and no data on their endostructural tooth structure have yet been published.

Here we examine the mandible fragment of an immature MUP individual from the Gargas cave (Aventignan, France, figure S1), found in 2011 during excavations led by two of us (see SI-1 for details). The Gargas mandible (hereafter GPA-646) was discovered associated with an accumulation of faunal remains, lithic elements, used pebbles and colouring materials, and was sealed in indurated sediment, all of which corresponds to a palimpsest of repeated domestic occupations that took place during the Middle Gravettian and are dated to between 33,000 and 28,300 cal BP (Foucher et al., 2011; 2012; 2019). GPA-646 itself is directly dated to ca. 29,000 cal BP (Foucher et al., 2019; see table S1). Shortly after its discovery, a preliminary description of GPA-646 was undertaken whilst a large part of the mandible was covered by indurated sediment and concretions (Foucher et al., 2012). From macroscopic observations of directly observable aspects, this preliminary description indicates that it is a relatively complete mandible (the right ramus being missing) of a young child between two and five years of age, with a possible abnormal swelling on the lateral side (Foucher et al., 2012). In the present study, we used both macroscopic observations of the mandible (after thorough cleaning of the calcitic coating partially covering it) and imaging techniques applied to an X-ray micro-computed tomography (microCT) record of GPA-646, to characterize the external and internal morphology of the mandible and its erupted and unerupted teeth. Our aims were:

i) to refine the age-at-death of this child and characterize its pattern of dental maturation;
ii) to comparatively assess the mandibular and dental morphology and dimensions;
iii) to quantify internal tissue proportions and enamel thickness of the deciduous first molar.

Methods

MicroCT acquisitions and preliminary treatment

In 2012, the two mandibular fragments were imaged at high resolution using the X8050-16 Viscom AG X-ray microcomputed tomography (microCT) equipment at the University of Poitiers. The scans were made using the following parameters: for the larger fragment GPA-646a, 150 kV voltage, 0.4 mA, 32 integrations per projection and a projection every 0.2°; for the smaller fragment GPA-646b, 90 kV voltage, 0.35 mA, 31.5 integrations per projection and a projection every 0.3°. Because of the presence of indurated sediment and a flat triangular pebble (ca. 8 cm for each side, and ca. 4.5 cm of thickness) firmly attached by a thin layer of concretion around the larger fragment GPA-646a (figures 1, S2), the resolution of its microCT record was lower than expected. The final volumes were reconstructed using DigiCT v.2.4.2 (DIGISENS) with an isotropic voxel size of 82.7 µm for GPA-646a and of 24.9 µm for GPA-646b. Subsequent 2D and 3D virtual imaging and morphometrics were performed at the IC2MP of the University of Poitiers and at the PACEA imaging laboratory of the University of Bordeaux. Around 50% of the lateral surface of the main fragment GPA-646a was originally covered by concretion. In 2015, this calcitic coating was nearly completely removed using gentle mechanical and chemical techniques (figure 1).

Methods of morphometric analysis

Macroscopic observations were made after removal of the thin layer of concretion on the main fragment. The linear measurements and angles followed the Martin (M-#) system (Bräuer, 1988), completed by measurements defined by Trinkaus (Trinkaus, 2002). They were taken either directly on the fragments or on the 3D model using Avizo, Fiji and TIVMI (Treatment and Increased Vision for Medical Imaging) software (see SI-4). The measurements on 3D models were repeated three times at least one week apart. As the differences between repeated measurements were negligible, the values obtained for each measurement were averaged and used in this study (table S5).

In order to virtually extract bone, teeth and dental tissues, semi-automatic threshold-based segmentation with manual corrections was conducted on the microCT record following the half-maximum height method (HMH, Spoor et al., 1993) and by taking repeated measurements on different slices of the virtual stack using Avizo 7.1 (Visualization Sciences Group Inc.). Because of the presence of indurated sediment and concretions around the larger fragment GPA-646a, the resolution of its microCT record was lower than expected, and the segmentation of the bone and teeth was technically difficult and time-consuming. While we were able to virtually segment and extract each tooth, an unambiguous distinction between enamel and dentine was not possible for this fragment (figures S2-S3), precluding any investigation of the dental tissue proportions for the GPA-646a fragment. On the other hand, no particular technical difficulties were encountered in segmenting the smaller fossil fragment GPA-646b, which is characterized by a rather distinct endostructural signal. In this case, the resolution of the microCT record is high enough to distinguish between tooth tissues. The study of dental tissue proportions was therefore conducted only on the smaller GPA-646b fragment. As only the LRdm1 has a complete crown on this fragment, this tooth is the only one for which we extracted dental tissue proportions and enamel thickness variables (see SI-4). The crown was digitally isolated from the roots (Olejniczak et al., 2008), and 3D surface models of the outer enamel surface (OES) and the enamel-dentine junction (EDJ) were generated using a constrained smoothing algorithm. The microCT record was used to examine the mineralization stage of each tooth, to assess molar crown morphological variation on both the OES and EDJ and to measure dental tissue proportions and enamel thickness. All the raw data obtained for the Gargas specimen are available in this paper and its supplementary information.

Bivariate plots of mandible dimensions, crown dimensions and dental tissue proportions were used to compare the morphometric characteristics of the Gargas mandible with those of the comparative specimens. A principal component analysis based on the mandible dimensions was performed for the specimens without missing data.

Comparative samples

Measurements obtained for the mandibular corpus, dental crown diameters, tissue proportions and enamel thickness were compared to those of Neandertals (Neand), Upper Palaeolithic modern humans (UPMH) and Holocene modern humans (HMH). Details of all comparative samples are provided in SI-5. For the mandible, the comparative sample comprised 90 immature specimens (table S6). For the permanent and deciduous teeth, the crown dimensions of GPA-646 were compared with those of 317 individuals (table S7). For the dental tissue proportions and enamel thickness of the LRdm1 of GPA-646, the comparative sample comprised 27 specimens (table S8).

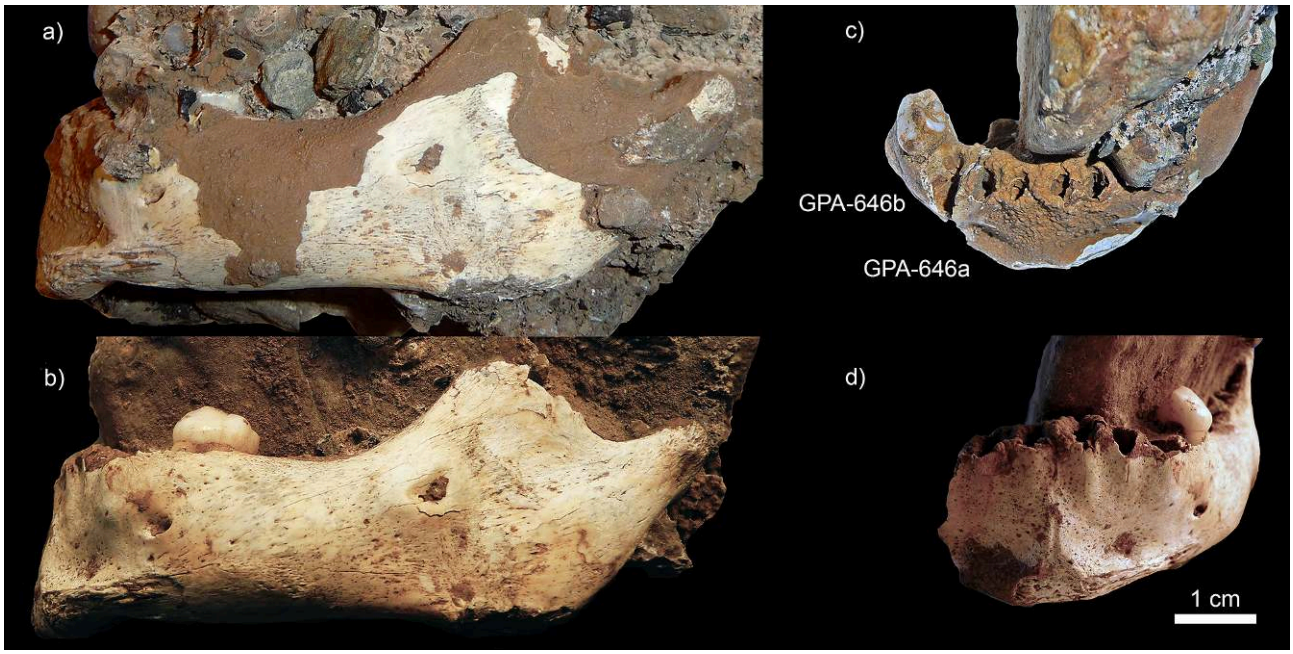

Figure 1. The Gargas mandible GPA-646. a) Left lateral view of GPA-646a before cleaning of the concretion and b) After cleaning. c) Supero-anterior view of GPA-646a and GPA-646b joined together. d) Anterior view of GPA-646a after cleaning / *La mandibule GPA-646 de Gargas. a) Vues latérales gauches de GPA-646a avant le nettoyage de la concrétion et b) Après le nettoyage. c) Vue supéro-antérieure de GPA-646a et GPA-646b réunis. d) Vue antérieure de GPA-646a après le nettoyage*

E. Trinkaus (Washington University) kindly provided most of the comparative data for the external measurements. Comparative data on dental tissue proportions and enamel thickness were acquired directly in this study.

Results and discussion

Current state of preservation of the mandibular corpus

The human immature mandible GPA-646 (figure 1) is now free of the thin layer of concreted sediment that covered around 50% of its lateral surface (figure 1a-b). It is composed of two mandibular fragments, GPA-646a and GPA-646b, that are joined along a longitudinal post-mortem fracture at the interdental septum of the right lateral incisor (LRdi2) and right deciduous canine (LRdc) (figure 1c). The larger fragment GPA-646a corresponds to the left half of the mandible and a small portion (ca. 1.5 cm) of the right half. The fragment is well preserved and only displays minor damage: the left coronoid process is missing, the left gonial angle is broken, and the condylar process and the inferior part of the symphyseal region are eroded (figure 1b,d). The lingual surface of GPA-646a is firmly attached to a flat triangular pebble by a thin layer of concretion (figures 1, S2). GPA-646b is a smaller fragment (22 × 14 mm) of the right half of the body (figures 1c, 2). Matrix infill of the cancellous bone is visible on the microCT record for both fragments (figures 2, S2).

Preservation and identification of the teeth

The left and right first deciduous molars (respectively LLdm1 and LRdm1) are the only erupted teeth still present on the mandible (figures 1-2). The alveoli of the six anterior deciduous teeth are empty (figures 1c-d, 2a). A portion of the enamel on the lingual and buccal surfaces of the LRdm1 has been lost. The germs of the right lateral permanent incisor (LRI2) and the right permanent canine (LRC) are visible in their crypts at the break between GPA-646a and GPA-646b. The microCT record allows identification of other unerupted tooth germs (figure 2): the central and lateral left permanent incisors (respectively LLI1 and LLI2), the right central permanent incisor (LRI1), a supernumerary incisor causing crowding in the anterior alveolar region (figures 2a-b, S3a), the left permanent canine (LLC), the right and left permanent third premolars (respectively LRP3 and LLP3), the left deciduous second molar (LLdm2, its occlusal surface being just at the alveolar margin) and the left permanent first molar (LLM1). Thus, a total of twelve teeth or germs are present on the GPA-646 mandible (see SI-2 for the complete description): the LRdm1, the LRP3 and the LRC are preserved in the fragment GPA-646b (figure 2c-d), whereas all the other teeth (including the supernumerary incisor) are preserved in the larger fragment GPA-646a (figure 2a-b).

The reported prevalence of supernumerary teeth in the permanent dentition of the living population ranges from 0.1% to 3.8% (Rajab and Hamdan, 2002). Cases in the lower incisor region are the least common, representing 0% to 5.1% of all supernumerary teeth identified (Rajab and Hamdan, 2002; Leco Berrocal et al., 2007; Celikoglu et al., 2010; Demiriz et al., 2015). The supernumerary tooth of GPA-646 therefore appears to be exceptional in the light of modern clinical data. Supernumerary teeth in the fossil record are also relatively rare and, interestingly, the other Eurasian Upper Pleistocene cases described so far are for one EUP and four MUP specimens from Russia, Moravia and south-western France (table S2). As heredity is believed to be an important etiological factor in the occurrence of supernumerary teeth, their presence in six European pre-LGM modern human individuals (including Gargas) – whereas no cases have been reported so far for older or later prehistoric groups – supports the hypothesis of a genetic singularity common to at least some EUP and MUP individuals. Interestingly, in several mammalian taxa, supernumerary teeth are found very frequently in hybrids (i.e. the product of interbreeding between individuals from genetically differentiated lineages: for a review, see Ackermann, 2010; Ackermann et al., 2019). Ackermann and colleagues wrote (2019: 97) that "*The consistency of these findings across taxa strongly suggests that the presence of such nonmetric traits in relatively high frequencies is a general indicator of hybridization*", and they indeed suggested this hypothesis for some of the MUP supernumerary tooth cases.

Maturation pattern and age-at-death

The symphysis of GPA-646 appears fully fused, both macroscopically and through microCT examination. Complete fusion of this region usually occurs during the first post-natal year in extant humans (Scheuer and Black, 2000). Only the deciduous teeth were erupted at the time of death of the Gargas child. Complete occlusion of the first deciduous molar and alveolar eruption of the second deciduous molar occur on average between 1 and 2 years in extant humans (AlQahtani et al., 2010). The dental mineralization stages (AlQahtani et al., 2010) for each tooth element of GPA-646 point to an age between 1 and 3 years (table S3). According to the results of the Bayesian analysis (table S4), the mineralization sequence (C/C/C/A/0/C/0) displayed by the permanent teeth of GPA-646 has a frequent occurrence in extant humans (see SI-3), and this specific mineralization sequence is shared with a girl aged 1.48 years. All the maturational aspects are compatible with an estimated age-at-death of 1 to 3 years for the Gargas child. Our assessment thus gives a slightly younger and narrower range for the age-at-death of this specimen than the previously published estimation.

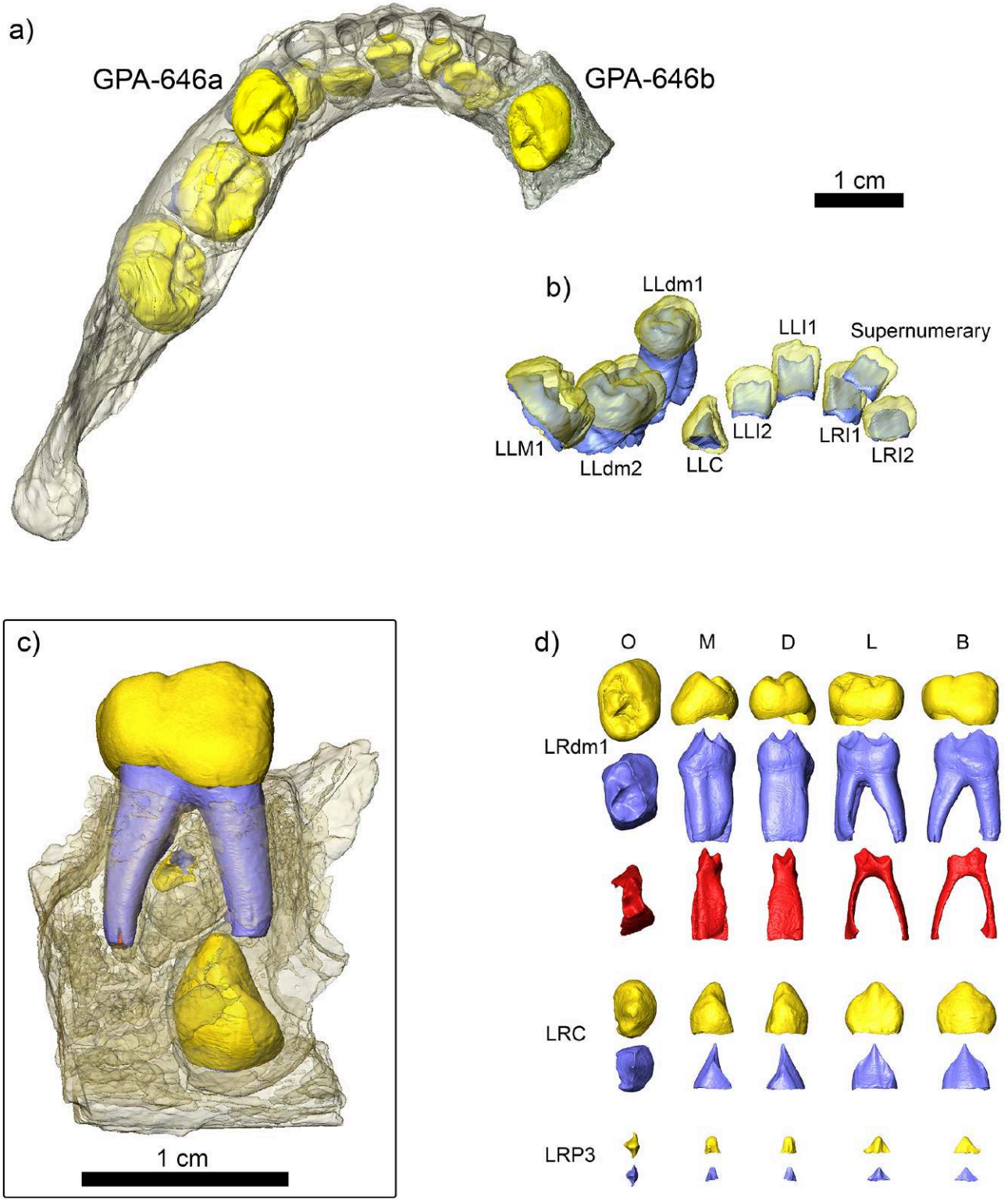

Figure 2. a) 3D rendering of GPA-646a and GPA-646b virtually joined together showing the bone (in semi-transparency) and the teeth in occlusal view, b) *In situ* deciduous and permanent teeth of GPA-646a in posterior view, c) Close-up of GPA-646b and its *in situ* teeth in right lateral view, d) Virtually extracted and 3D rendered deciduous and permanent tooth elements of GPA-646b in occlusal (O), mesial (M), distal (D), lingual (L) and buccal (B) views. Enamel appears in yellow, dentine in blue, and the pulp cavity in red / *a) Rendu 3D de GPA-646a et GPA-646b réunis virtuellement montrant l'os (en semi-transparence) et les dents en vue occlusale, b) Dents déciduales et permanentes incluses de GPA-646a en vue postérieure, c) Gros plan sur GPA-646b et ses dents incluses en vue latérale droite, d) Éléments dentaires déciduaux et permanents extraits virtuellement et rendus 3D de GPA-646b en vues occlusale (O), mésiale (M), distale (D), linguale (L) et buccale (B). L'émail apparait en jaune, la dentine en bleu et la cavité pulpaire en rouge*

Mandibular morphometric analysis

The mandibular dimensions for GPA-646 and the comparative samples are given in table 1 (see also table S9). The external cortical surface of all of the bone is highly porous, as is typically seen in very young individuals. A clear chin is observable on its anterior surface (figure 1), formed by a mental protuberance (*tuber symphyseos*), ca. 11 mm in width, that continues laterally on each side as a thickening of the inferior margin of the corpus, forming an inverted ''T''-shaped structure. To each side of the mental protuberance lies a well-marked depression (*incisura mandibulae anterior*). Even though the inferior part of the area is eroded, this morphology clearly corresponds to the derived modern human anterior symphysis (*mentum osseum* stage 5 – Dobson and Trinkaus, 2002), which does not occur in Neandertals or in other late archaic humans (Schwartz and Tattersall, 2000; Dobson and Trinkaus, 2002; Liu et al., 2010).

The symphysis dimensions are relatively small (table 1), especially the height of the symphysis compared to those of El Castillo 2 and Lagar Velho 1 (figure 3a). The lateral corpus decreases slightly in height from the symphysis to the ramus (figure 1; table 1). A single ovoid (ca. 2.0 mm in breadth and 1.0 mm in height) mental foramen is visible on each side (figure 1), directly below the anterior root of the LLdm1. This position is common for immature Neandertal and UP individuals with only deciduous teeth erupted (Coqueugniot, 2000). The corpus does not appear extremely robust at the mental foramen compared to Neandertal individuals at a similar stage of maturation (Arnaud, 2015). More posteriorly on the lateral surface of the mandible, a distinctive bulge is present around the crypt of the LLM1 (figures 1b, S2b). Previously described as abnormal (Foucher et al., 2012), this bulging shape appears to be directly linked to the developing tooth germ contained within it. The ramus is low compared to the corpus. The gonial angle is ca. 150° (figure 1; table S9), which is consistent with the general stage of maturation (in extant humans the gonial angle is usually between 150 and 130° before complete eruption of the deciduous dentition (Jensen and Palling, 1954). Unfortunately, the medial surface of the ramus is firmly attached to the block, precluding any direct observations, but based on the 3D model no prominent relief was detected, such as a medial pterygoid tubercle frequently found in Neandertals and in some Early and Middle Pleistocene specimens (Rak et al., 1994; 1996; Bermúdez de Castro et al., 2015). The condyle is medially placed relative to the crest of the mandibular notch (score II, Jabbour et al., 2002), which is common in recent *Homo sapiens* of a similar age (Jabbour et al., 2002). The dental arcade of GPA-646 appears wide (table 1). The bi-external deciduous canine and first molar breadths (figure 3b-d) are well above the mean values for both UPMH and HMH (table 1; figure S4). In particular, both values for dimensions are higher than the maximum values for UPMH individuals with only deciduous teeth erupted and recent Europeans aged 1 to 3 years, and are roughly similar to Neandertal values (figures 3d, S5). While the two corpus dimensions show an overlap between Neandertals and modern humans (figure S6), it has been shown that plotting mandibular breadth against lateral corpus height clearly distinguishes Neandertals from early modern humans (Verna et al., 2012). Interestingly, the morphology of GPA-646 appears to be closer to that of Neandertals than other UPMH children (figures 3b, S5), i.e. a broad mandible compared to its height. Despite the Gargas child being very young, its mandible displays large breadth dimensions (figure 3b-c) that are comparable to Neanderthal specimens. The results of the principal component analysis based on these six mandibular variables (figure 4) confirm that the Gargas mandible differs from contemporaneous specimens: the Gargas mandible appears to be closer to the morphology of Neandertals, while other MUP specimens display a morphology that is similar to the Holocene sample (figure 4).

	Symphysis height	Symphysis breadth	Bi-external dc arcade breadth	Bi-external dm1 arcade breadth	Corpus dm1-dm2 height	Corpus dm1-dm2 breath
GPA-646	20.1*	10.4*	32.1*	40.8*	17.2*	11.4*
Neand	21.7 ± 2.0 [19.0-25.7] n=10	12.0 ± 1.5 [9.7-14.0] n=8	32.4 ± 1.8 [30.1-35.2] n=9	43.4 ± 1.8 [41.5-46.0] n=7	18,8 ± 2.6 [15.2-22.8] n=11	12,2 ± 1.1 [10.3-14.2] n=11
UPMH	21.8 ± 1.9 [19.4-25.1] n=11	11.0 ± 1.2 [9.6-13.3] n=10	29.3 ± 1.0 [28.2-30.8] n=5	38.3 ± 2.0 [36.1-40.0] n=3	19.2 ± 2.5 [16.5-21.9] n=4	11.4 ± 0.5 [10.8-12.1] n=4
HMH	20.9 ± 2.2 [15.1-24.4] n=30	11.1 ± 1.0 [8.9-13.0] n=30	25.8 ± 2.3 [20.6-31.0] n=30	36.0 ± 2.3 [31.6-39.9] n=30	17.1 ± 2.0 [11.7-21.8] n=30	10.3 ± 0.9 [8.7-12.5] n=30

Values are in mm. The data for the comparative samples is presented as mean ± standard deviation; minimum and maximum values are in brackets; *n* indicates sample size. *: Measured on the 3D models. Individuals included in the comparative samples are only those with erupted deciduous teeth (S1 according to Verna et al., 2012).

Table 1. Mandibular dimensions for GPA-646 and the comparative samples of Neandertals (Neand), Upper Palaeolithic (UPMH) and Holocene (HMH) modern humans / *Dimensions mandibulaires de GPA-646 et de l'échantillon comparatif d'individus Néandertaliens (Neand), du Paléolithique supérieur (UPMH) et de l'Holocène (HMH)*

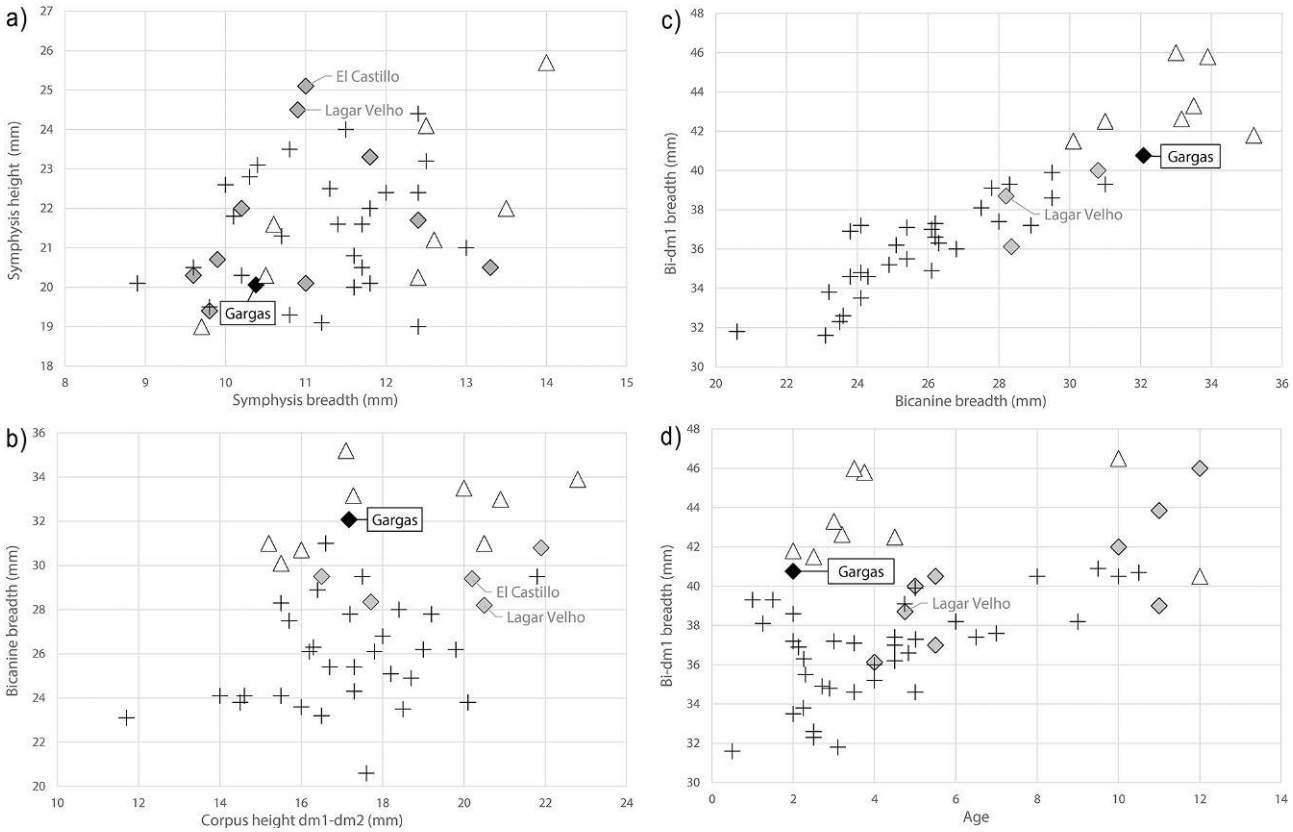

Figure 3. Bivariate plots of the mandibular dimensions of Gargas compared to the values for Neandertals (triangles), Upper Palaeolithic (diamonds) and Holocene modern humans (crosses) for a) Symphysis breadth and height, b) Corpus height and bicanine breadth, c) Bicanine breadth and bi-dm1 breadth (with only comparative S1 specimens for a, b and c, see SI-6) and d) bi-dm1 breadth against age (with all immature specimens) / *Graphiques bivariés des dimensions mandibulaires de Gargas comparées aux valeurs des individus Néandertaliens (triangles), du Paléolithique supérieur (losanges) et de l'Holocène (croix) pour a) La largeur et la hauteur de la symphyse, b) La hauteur du corps et la largeur bicanine, c) La largeur bicanine et la largeur bi-dm1 (avec seulement les individus S1 pour a, b et c, voir SI-6) et d) La largeur bi-dm1 selon l'âge (avec tous les individus immatures)*

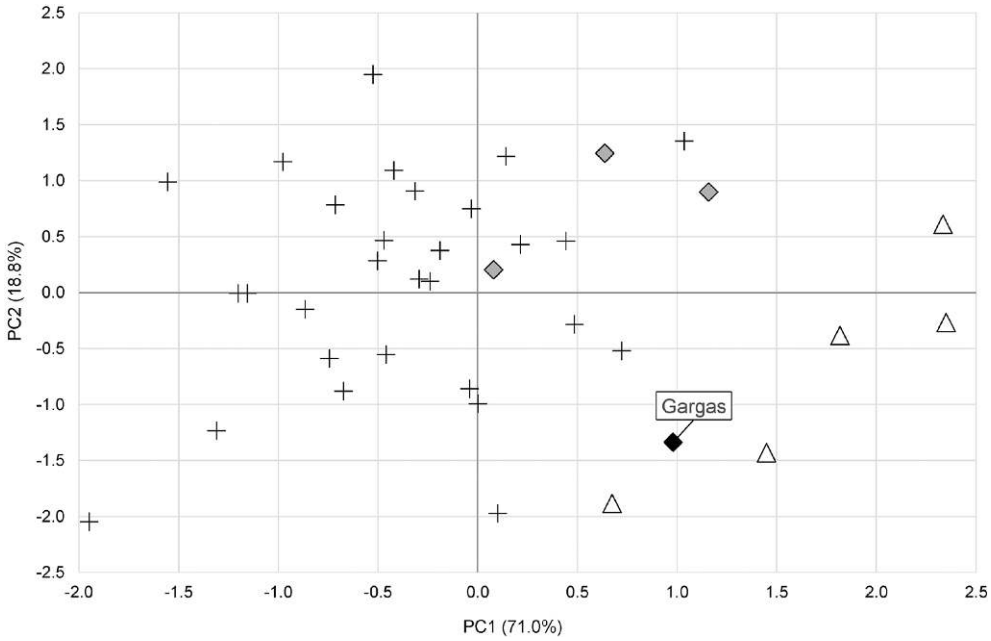

Figure 4. Results of the principal component analysis for the mandibular dimensions (see table 1) of Gargas compared to Neandertals (triangles), Upper Palaeolithic (diamonds) and Holocene modern humans (crosses) / *Résultats de l'analyse en composantes principales pour les dimensions mandibulaires (voir tableau 1) de Gargas comparé aux individus Néandertaliens (triangles), du Paléolithique supérieur (losanges) et de l'Holocène (croix)*

It has been suggested that the large breadth of the dental arcade in Middle Palaeolithic fossils may be related to large anterior dental dimensions (Mallegni and Trinkaus, 1997). This hypothesis can be rejected for GPA-646, as its anterior teeth are not especially large (see infra). It seems possible that the morphology of the GPA-646 arcade is the by-product of the presence of a supernumerary tooth in the incisor region. In any case, the proportions of the GPA-646 mandible appear to be "archaic", i.e. closer to the earlier groups (Neandertals and MPMH) than to UPMH (including the contemporaneous Lagar Velho 1 and El Castillo 2 specimens) or the comparative Holocene sample. This result is not surprising considering that previous analyses have shown the presence of such "archaic" traits in early modern human specimens from Europe, Asia and Africa (Trinkaus et al., 2003; Crevecoeur and Trinkaus, 2004; Shang and Trinkaus, 2010). These traits have been used to underline that the biological processes through which humans became "modern" were more complex than usually thought and/or reflect admixture between modern human and regional late archaic human groups (Trinkaus et al., 2003; Shang and Trinkaus, 2010).

Dental morphometric analysis

Dental non-metric scores for the deciduous and permanent molars (see SI-7) reveal that no supplementary cusps are present in GPA-646 and the hypoconulid on the LLM1 is small (table S10). The morphology of the deciduous and permanent molars as observed on both the outer enamel surface (OES) and the enamel-dentine junction (EDJ) appears simple, especially compared to more recent Upper Palaeolithic individuals (from Lafaye and La Marche, see Le Luyer, 2016). Overall, the morphology of the Gargas teeth displays modern characteristics.

Crown mesiodistal and buccolingual diameters for GPA-646 and the comparative samples are provided in table 2. The dimensions for the anterior permanent teeth of GPA-646 fall within the variability of the comparative samples and are closer to the mean values for UPMH specimens. Conversely, the crown dimensions of the GPA-646 deciduous and permanent molars are very large (figure 5), larger than the averages obtained for the Neandertal, UPMH, and HMH samples (table 2). GPA-646 is especially impressive for the mesiodistal diameter of its deciduous molars (figure 5): the values for the left and right Ldm1s exceed all the individual values from the comparative samples, and the value for the Ldm2 is only equalled and exceeded by two EUP specimens. Both deciduous and permanent molars of GPA-646 display larger mesiodistal dimensions than the two other contemporary immature Lagar Velho 1 and El Castillo 2 specimens (figure 5). For the buccolingual dimensions, only the Ldm1s of GPA-646 clearly exceed those of Lagar Velho 1 and El Castillo 2 (figure 5a) while the Ldm2 and LM1 of the three MUP immature specimens show relatively similar buccolingual dimensions (figure 5b-c).

UP individuals (including Lagar Velho 1 and El Castillo 2) tend to display relatively large deciduous and permanent molars, but their dimensions remain smaller on average than those of the Gargas child. Indeed, the deciduous molars of GPA-646 exhibit crown dimensions that are rarely seen, if at all, in the entire UP sample. Interestingly, greater tooth size has been considered as a possible indicator of hybrids in non-human primates (Jolly et al., 1997; Ackermann, 2010). The unusual dental dimensions of the Gargas molars may thus be related to undescribed admixtures of different early European populations of anatomically modern humans or, less likely considering the direct date obtained for GPA-646, to interactions between late Neandertals and early modern

	Mesiodistal crown diameters							**Buccolingual crown diameters**		
	Super-numerary	LI1	LI2	LC	Ldm1	Ldm2	LM1	Ldm1	Ldm2	LM1
GPA-646 left		(5.5)*	(6.0)*	(7.1)*	9.7**	11.5*	12.3*	7.6*	9.6*	11.3*
GPA-646 right	(5,3)*	(5.4)*	(6,1)*		9.6**			7.9**		
Neand		5.5 ± 0.5 [4.4-6.5] n=12	6.5 ± 0.5 [5.8-7.4] n=25	7.8 ± 0.4 [6.8-8.5] n=31	8.7 ± 0.4 [8.1-9.6] n=22	10.3 ± 0.5 [9.2-11.1] n=27	11.4 ± 0.6 [10.2-12.5] n=40	7.4 ± 0.5 [6.4-8.6] n=24	9.3 ± 0.5 [9.0-10.2] n=28	10.8 ± 0.5 [9.5-11.8] n=55
UPMH		5.6 ± 0.5 [4.0-6.5] n=19	6.3 ± 0.4 [5.0-7.3] n=25	7.2 ± 0.7 [6.1-9.0] n=25	8.6 ± 0.6 [7.3-9.5] n=32	10.5 ± 0.6 [9.3-11.6] n=47	11.5 ± 0.8 [8.0-13.0] n=80	7.2 ± 0.4 [6.1-8.1] n=40	9.2 ± 0.6 [7.7-10.5] n=58	11.1 ± 0.8 [6.8-13.0] n=98
HMH		5.2 ± 0.5 [4.6-6.4] n=31	5.6 ± 0.4 [4.8-7.0] n=50	6.7 ± 0.4 [5.5-8.8] n=49	8.0 ± 0.7 [6.8-9.0] n=13	9.9 ± 0.6 [8.8-10.8] n=17	11.1 ± 0.7 [9.3-12.7] n=56	7.1 ± 0.3 [6.3-7.7] n=20	9.0 ± 0.4 [8.3-9.9] n=21	10.6 ± 0.5 [9.4-12.0] n=82

Values are in mm. (##) indicates a measurement with small degree of estimation. *: Measured on the 3D models. **: Measured both on the 3D models and directly on the fossil. The data for the comparative samples is presented as mean ± standard deviation: minimum and maximum values are in brackets, *n* indicates sample size

Table 2. Dental crown dimensions for GPA-646 and the comparative samples of Neanderthals (Neand), Upper Palaeolithic (UPMH) and Holocene modern humans (HMH) / *Dimensions des couronnes dentaires de GPA-646 et de l'échantillon comparatif d'individus Néandertaliens (Neand), du Paléolithique supérieur (UPMH) et de l'Holocène (HMH)*

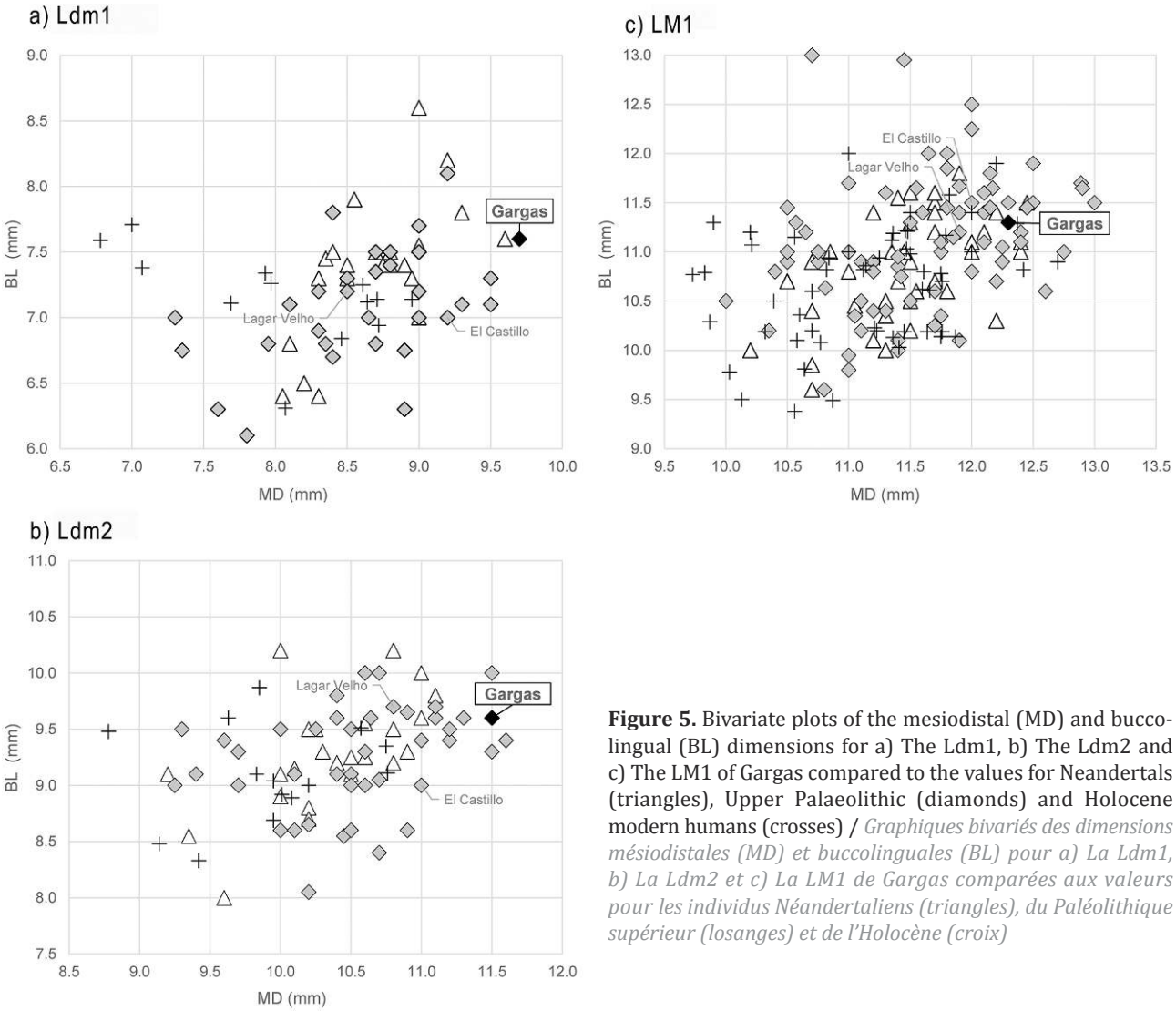

Figure 5. Bivariate plots of the mesiodistal (MD) and buccolingual (BL) dimensions for a) The Ldm1, b) The Ldm2 and c) The LM1 of Gargas compared to the values for Neandertals (triangles), Upper Palaeolithic (diamonds) and Holocene modern humans (crosses) / *Graphiques bivariés des dimensions mésiodistales (MD) et buccolinguales (BL) pour a) La Ldm1, b) La Ldm2 et c) La LM1 de Gargas comparées aux valeurs pour les individus Néandertaliens (triangles), du Paléolithique supérieur (losanges) et de l'Holocène (croix)*

humans. In any case, our study of GPA-646 confirms that the phenotypical diversity of the European pre-LGM modern human fossil sample tends to be very high (Zilhão and Trinkaus, 2002; Teschler-Nicola, 2006; Trinkaus et al., 2012). Previous studies have reported a significant decrease in crown size for permanent molars (expressed for both diameters) between pre and post-LGM groups (Brace, 1967; Frayer, 1977). When plotted against chronological variables (i.e. C^{14} dates; figure S7), the LM1, Ldm1, and Ldm2 crown dimensions of the UPMH specimens included in this study do not appear to follow this trend and no decrease in crown sizes between 15,000 and 10,000 BP has been identified. Indeed, greater LM1 dimensions are present in the MUP and in the terminal phase of the LUP (figure S7), and while a slight decrease seems noticeable for the deciduous molars, no clear trends over time are identified as large teeth are also shown to occur at the end of the UP (figure S7). However, geographical patterns have emerged from our analysis: the Ldm2 dimensions of (south)-western European UP fossils appear to be larger than those of (north)-eastern UP specimens (table S11). Similar results have been obtained with a subsample of specimens dated between 45,000 and 20,000 BP, and this trend is also seen for the MUP only, although the sample size is relatively small (table S11). Our analysis is the first to report such a geographical pattern for UP dental dimensions. GPA-646, as an MUP specimen from western Europe, thus presents extreme dental dimensions that nevertheless fit broader, and previously undescribed, chronological and geographical patterns. As tooth crown size is governed by genetic, epigenetic and environmental factors (see Hughes and Townsend, 2013 for a review), our results suggest complex interactions of these factors through the European UP and may indicate distinct populations during the MUP, not identified on the basis of cranial morphology (Mounier et al., 2020). Further analyses are required in order to clarify these interactions.

Enamel thickness and tissue proportions

The internal dental characteristics of GPA-646 have very high values (tables 3-4): the enamel area and volume of its LRdm1 exceed all of the individual values from the comparative samples (figure S8). Moreover, its crown area and volume and its EDJ length and area exceed those of the other modern humans and are more similar to Neandertal values. However, the tissue proportions within the crown sets GPA-646 apart from Neandertals, with particularly high values for enamel area and volume but lower dentine and pulp values (figure S8). Therefore, the LRdm1 of GPA-646 exhibits a pattern closer to UPMH individuals with a low percentage of the crown volume and area that is dentine and pulp, and high AET and RET values both in 3D and 2D. The visual representation of the RET (figure 6), clearly distinguishing Neandertals from modern human specimens, shows the Gargas LRdm1 to be closer to the latter group but at an extreme position, especially for 2D variables (figure 6b).

Enamel thickness can change rapidly over short evolutionary periods (Alvesalo and Tigerstedt, 1974; Potter et al., 1976; Hlusko et al., 2004; Horvath et al., 2014) and a thick enamel is associated with strong masticatory forces (Schwartz, 2000; Lucas et al., 2008). It may therefore be suggested that the high enamel thickness in GPA-646 indicates high biomechanical loads for this MUP population. Endostructural analyses of other MUP teeth from south-western France are required in order test this hypothesis.

Conclusion

The GPA-646 mandible belongs to an MUP child who died between 1 and 3 years of age. Its characteristics differ from the two other contemporaneous individuals from western Europe, namely Lagar Velho 1 from Portugal and El Castillo 2 from Spain. The Gargas child displays modern morphological traits, such as a true chin and a modern pattern of dental maturation. However, our examination of both external and internal characteristics reveals that this Late Pleistocene child possessed a robust mandible with a wide dental arcade. The deciduous molars are large and have an enamel quantity exceeding all reported values so far for modern humans. It also displays a very rare condition, namely a supernumerary lower permanent incisor, which can be added to the list of Late Pleistocene congenital disorders and rare anomalies. Interestingly, these last two conditions have been identified as possible indicators of hybridization in the human fossil record (Harvati et al., 2007; Ackermann, 2010; Ackermann et al., 2019), and their presence in GPA-646 may indicate large-scale movements of individuals from previously isolated populations during the EUP and/or the MUP. Moreover, the differences identified between the three contemporaneous MUP immature individuals from Spain, Portugal and France raise the question of MUP biological variability and the subsequent role of genetic, epigenetic, and environmental factors.

	Crown volume (mm^3)	Enamel volume (mm^3)	Coronal dentine and pulp volume (mm^3)	Crown volume that is dentine and pulp (%)	EDJ area (mm^2)	3D AET (Average Enamel Thickness) (mm)	3D RET (Relative Enamel Thickness)
GPA-646-LRdm1	202.0	78.6	123.4	61.1	119.6	0.7	13.2
Neand (n=7)	211.2 ± 33.8	56.2 ± 13.9	155.0 ± 21.7	73.7 ± 3.6	132.8 ± 20.1	0.4 ± 0.1	7.8 ± 1.1
UPMH (n=4)	161.5 ± 26.2	58.6 ± 15.9	102.9 ± 10.9	64.1 ± 4.7	103.6 ± 14.4	0.6 ± 0.1	12.0 ± 1.6
HMH (n=16)	149.4 ± 22.4	50.4 ± 11.1	99.0 ± 17.2	66.2 ± 5.9	97.4 ± 15.0	0.5 ± 0.1	11.3 ± 2.3

The data for the comparative samples are presented as "mean ± standard deviation".

Table 3. 3D dental tissue proportions and enamel thickness of the LRdm1 for GPA-646 and the comparative samples of Neandertals (Neand), Upper Palaeolithic (UPMH) and Holocene modern humans (HMH) / *Proportions des tissus dentaires en 3D et épaisseur de l'émail de la LRdm1 de GPA-646 et de l'échantillon comparatif d'individus néandertaliens (Neand), du Paléolithique supérieur (UPMH) et de l'Holocène (HMH)*

	Crown area (mm^2)	Enamel area (mm^2)	Coronal dentine and pulp area (mm^2)	Crown area that is dentine and pulp (%)	EDJ length (mm)	2D AET (Average Enamel Thickness) (mm)	2D RET (Relative Enamel Thickness)
GPA-646-LRdm1	39.4	10.7	28.7	72.9	16.5	0.7	12.1
Neand (n=7)	38.2 ± 4.1	6.7 ± 1.1	31.5 ± 3.1	82.6 ± 1.4	16.8 ± 1.3	0.4 ± 0.1	7.0 ± 0.5
UPMH (n=4)	34.4 ± 2.5	8.2 ± 1.3	26.2 ± 1.2	76.3 ± 2.1	16.1 ± 0.8	0.5 ± 0.1	9.9 ± 0.9
HMH (n=16)	29.6 ± 4.4	6.9 ± 1.1	22.8 ± 3.5	76.8 ± 2.1	14.5 ± 1.7	0.5 ± 0.1	10.1 ± 1.4

The data for the comparative samples are presented as "mean ± standard deviation".

Table 4. 2D dental tissue proportions and enamel thickness of the LRdm1 for GPA-646 and the comparative samples of Neandertals (Neand), Upper Palaeolithic (UPMH) and Holocene modern humans (HMH) / *Proportions des tissus dentaires en 2D et épaisseur de l'émail de la LRdm1 de GPA-646 et de l'échantillon comparatif d'individus néandertaliens (Neand), du Paléolithique supérieur (UPMH) et de l'Holocène (HMH)*

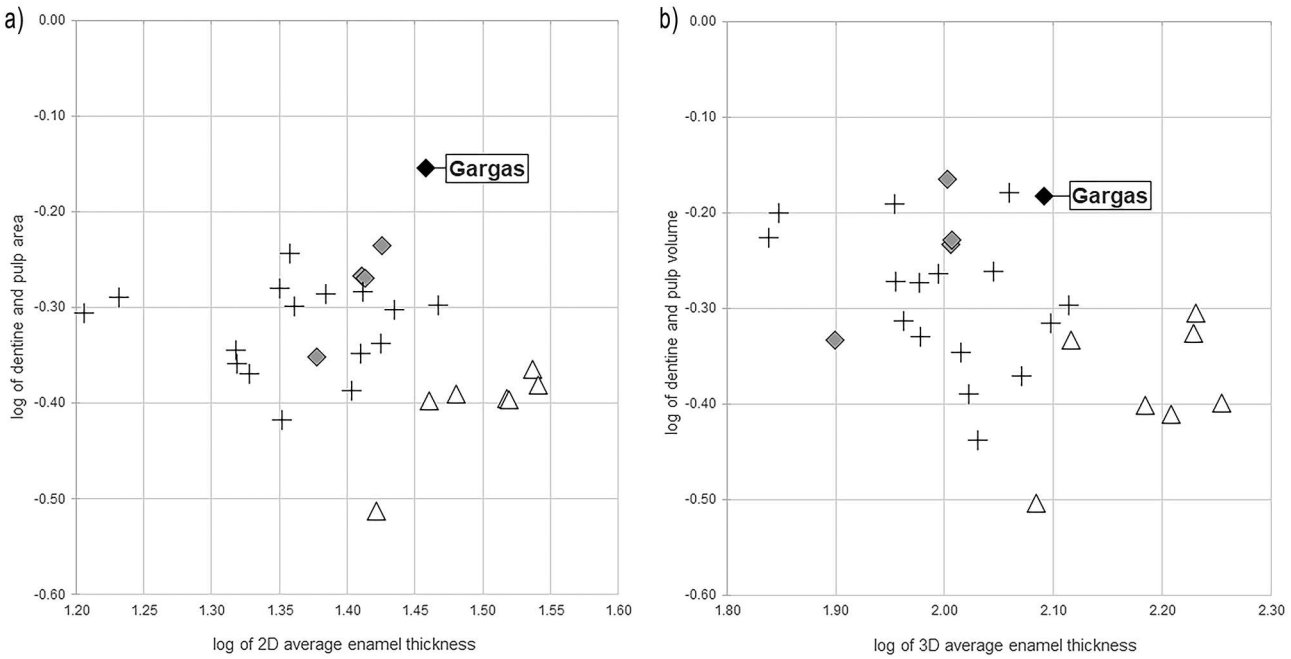

Figure 6. Bivariate plots of the internal proportions of the LRdm1 of Gargas compared to values for Neandertals (triangles), Upper Palaeolithic (diamonds) and Holocene modern humans (crosses). a) 3D average enamel thickness (log) against crown dentine and pulp volume (log) and b) 2D average enamel thickness (log) against crown dentine and pulp area (log) / *Graphiques bivariés pour les proportions internes de la LRdm1 de Gargas comparées aux valeurs pour les individus Néandertaliens (triangles), du Paléolithique supérieur (losanges) et de l'Holocène (croix). a) Épaisseur moyenne de l'émail en 3D (log) contre le volume de dentine et de pulpe dans la couronne (log) and b) Épaisseur moyenne de l'émail en 2D (log) contre l'aire de la dentine et de la pulpe dans la couronne (log).*

Acknowledgements

Thanks to the municipality of Aventignan, the owner of the cave, and the not-for-profit organizations "*Archéologies*" and "*Association pour le Rayonnement de l'Art Pariétal Européen*" for their help during our excavations. Thanks also to Monique Drieux (Materia Viva) for her help during the cleaning of the fossil. SV thanks Dominique Henry-Gambier (University of Bordeaux, CNRS, UMR 5199 PACEA) for giving him the opportunity to study this fossil. Thanks to Arnaud Mazurier (CNRS, UMR 7285 IC2MP) for the acquisition of the 3D data and to Erik Trinkaus (Washington University) for sharing his data and for his helpful comments on the manuscript.

This research was funded by the French National Research Agency (ANR GRAVETT'OS, ANR-15-CE33-0004). The excavations in Gargas were funded by the French Ministry of Culture (*DRAC Occitanie*) with support from the Hautes-Pyrénées *département* council. MLL's work was supported by the European Union's Horizon 2020 research and innovation program under the Marie Skłodowska-Curie grant agreement no. 796499.

Supplementary information

Supplementary information are available online at: https://journals.openedition.org/bmsap/9853?file=1

References

Ackermann RR (2010) Phenotypic traits of primate hybrids: recognizing admixture in the fossil record. Evolutionary Anthropology 19:258-270 [https://doi.org/10.1002/evan.20288]

Ackermann RR, Arnold ML, Baiz MD et al (2019) Hybridization in human evolution: Insights from other organisms. Evolutionary Anthropology 28(4):189-209 [https://doi.org/10.1002/evan.21787]

AlQahtani SJ, Hector MP, Liversidge HM (2010) Brief communication: The London atlas of human tooth development and eruption. American Journal of Physical Anthropology 142(3): 481-490 [https://doi.org/10.1002/ajpa.21258]

Alvesalo L, Tigerstedt PMA (1974) Heritabilities of human tooth dimensions. Hereditas 77(2):311-318 [https://doi.org/10.1111/j.1601-5223.1974.tb00943.x]

Arnaud J (2015) La mandibule d'Archi 1 : Étude morphologique et morphométrique détaillée d'un néandertalien immature. Bulletins et Mémoires de la Société d'Anthropologie de Paris 27(1-2): 42-55 [https://doi.org/10.1007/s13219-014-0096-z]

Bayle P, Macchiarelli R, Trinkaus E et al (2010) Dental maturational sequence and dental tissue proportions in the early Upper Paleolithic child from Abrigo do Lagar Velho, Portugal. Proceedings of the National Academy of Sciences of the United States of America 107(4):1338-1342 [https://doi.org/10.1073/pnas.0914202107]

Benazzi S, Douka K, Fornai C et al (2011) Early dispersal of modern humans in Europe and implications for Neanderthal behaviour. Nature 479(7374):525-528 [https://doi.org/10.1038/nature10617]

Bermúdez de Castro J-M, Quam R, Martinón-Torres M et al (2015) The medial pterygoid tubercle in the Atapuerca Early and Middle Pleistocene mandibles: Evolutionary implications: Medial Pterygoid Tubercle in Atapuerca. American Journal of Physical Anthropology 156(1):102-109 [https://doi.org/10.1002/ajpa.22631]

Brace CL (1967) Environment, tooth form and size in the Pleistocene. Journal of Dental Research 46(5):809-816

Bräuer G (1988) Osteometrie In: Knußmann R, Schwidetzky I, Jürgens HW, Ziegelmayer G (eds) Anthropologie Handbuch der vergleichenden Biologie des Menschen. Gustav Fischer Verlag Stuttgart, New York, pp 160-232

Celikoglu M, Kamak H, Oktay H (2010) Prevalence and characteristics of supernumerary teeth in a non-syndrome Turkish population: Associated pathologies and proposed treatment. Medicina Oral Patología Oral y Cirugia Bucal:e575-e578 [https://doi.org/10.4317/medoral.15.e575]

Coqueugniot H (2000) La position du foramen mentonnier chez l'enfant : Révision ontogénétique et phylogénétique. Bulletins et Mémoires de la Société d'Anthropologie de Paris 12(3-4): 227-246

Cevecoeur I, Trinkaus E (2004) From the Nile to the Danube: a comparision of the Nazlet Khater 2 and Oase 1 Early modern human mandibles. ANTHROPOLOGIE 42(3):203-214 [http://www.jstor.org/stable/26292696]

Demiriz L, Durmuslar M, Misir A (2015) Prevalence and characteristics of supernumerary teeth: A survey on 7348 people. Journal of International Society of Preventive and Community Dentistry 5(7):39 [https://doi.org/10.4103/2231-0762.156151]

Foucher P, San Juan-Foucher C, Henry-Gambier D et al (2012) Découverte de la mandibule d'un jeune enfant dans un niveau gravettien de la grotte de Gargas (Hautes-Pyrénées, France) / Discovery of the mandible of a young child in a Gravettian level of Gargas cave (Hautes-Pyrenees, France). PALEO 23: 323-336 [https://doi.org/10.4000/paleo.2472]

Foucher P, San Juan-Foucher C, Oberlin C (2011) Les niveaux d'occupation gravettiens de Gargas (Hautes-Pyrénées) : nouvelles données chronostratigraphiques In: Goutas N, Guillermin P, Klaric L, Pesesse D, Goutas N, Guillermin P, Klaric L, Pesesse D (eds) À la recherche des identités gravettiennes: actualités, questionnements et perspectives, Actes de la table ronde sur le Gravettien en France et dans les pays limitrophes. Société Préhistorique française, Paris, pp 209-216

Foucher P, San Juan-Foucher C, Villotte S et al (2019) Les vestiges humains gravettiens de la grotte de Gargas (Aventignan, France) : datations 14C AMS directes et contexte chrono-culturel. Bulletin de la Société préhistorique Française 116(1):29-39

Frayer DW (1977) Metric dental change in the European Upper Paleolithic and Mesolithic. American Journal of Physical Anthropology 46(1):109-120

Fu Q, Posth C, Hajdinjak M et al (2016) The genetic history of Ice Age Europe. Nature 534(7606):200-205 [https://doi.org/10.1038/nature17993]

Garralda MD, Maíllo-Fernández JM, Higham T et al (2019) The Gravettian child mandible from El Castillo Cave (Puente Viesgo, Cantabria, Spain). American Journal of Physical Anthropology 170(3):331-350 [https://doi.org/10.1002/ajpa. 23906]

Harvati K, Gunz P, Grigorescu D (2007) Cioclovina (Romania): affinities of an early modern European. Journal of Human Evolution 53(6):732-746 [https://doi.org/10.1016/j.jhevol.2007.09.009]

Henry-Gambier D (2008a) Comportement des populations d'Europe au Gravettien : pratiques funéraires et interprétatons. PALEO 20:165-204 [https://doi.org/10.4000/paleo.1632]

Henry-Gambier D (2008b) Les sujets juvéniles du Paléolithique supérieur d'Europe à travers l'analyse des sépultures primaires : l'exemple de la culture gravettienne In: Gusi i Jener F, Muriel S, Olaria i Puyoles C (eds) Nasciturus: infans, puerulus Vobis mater terra La muerte en la infancia. Diputació de Castelló, Servei d'Investigacions Arqueològiques i Prehistòriques, Castelló, pp 331-364

Higham T, Compton T, Stringer C et al (2011) The earliest evidence for anatomically modern human in northwestern Europe. Nature 479(7374):521-524 [https://doi.org/10.1038/nature10484]

Hlusko LJ, Suwa G, Kono RT et al (2004) Genetics and the evolution of primate enamel thickness: a baboon model. American Journal of Physical Anthropology 124(3):223-233 [https://doi.org/10.1002/ajpa.10353]

Holt BM, Formicola V (2008) Hunters of the Ice Age: The biology of Upper Paleolithic people. American Journal of Physical Anthropology 47(Suppl):70-99 [https://doi.org/10.1002/ajpa. 20950]

Horvath JE, Ramachandran GL, Fedrigo O et al (2014) Genetic comparisons yield insight into the evolution of enamel thickness during human evolution. Journal of Human Evolution 73: 75-87 [https://doi.org/10.1016/j.jhevol.2014.01.005]

Hublin JJ, Sirakov N, Aldeias V et al (2020) Initial Upper Palaeolithic Homo sapiens from Bacho Kiro Cave, Bulgaria. Nature 581 (7808):299-302 [https://doi.org/10.1038/s41586-020-2259-z]

Hughes TE, Townsend GC (2013) Twin and family studies of human dental crown morphology: genetic, epigenetic, and environmental determinants of the modern human dentition. In: Scott GR, Irish JD (eds) Anthropological perspectives on tooth morphology: genetics, evolution, variation. Cambridge University Press, Cambridge, pp 31-68

Jabbour RS, Richards GD, Anderson JY (2002) Mandibular condyle traits in Neanderthals and other Homo: A comparative, correlative, and ontogenetic study. American Journal of Physical Anthropology 119(2):144-155 [https://doi.org/10.1002/ajpa.10108]

Jensen E, Palling M (1954) The gonial angle. American Journal of Orthodontics 40(2):120-133 [https://doi.org/10.1016/0002-9416(54)90127-x]

Jolly CJ, Woolley-Barker T, Beyene S et al (1997) Intergeneric Hybrid Baboons. International Journal of Primatology 18(4): 597-627 [https://doi.org/10.1023/A:1026367307470]

Le Luyer M (2016) Évolution dentaire dans les populations humaines de la fin du Pléistocène et du début de l'Holocène (19000-5500 cal. BP) : une approche intégrée des structures externe et interne des couronnes pour le Bassin aquitain et ses marges., Ph.D. thesis, Université de Bordeaux, 456 p

Leco Berrocal MI, Martín Morales JF, Martínez González JM (2007) An observational study of the frequency of supernumerary teeth in a population of 2000 patients. Medicina Oral, Patologia Oral Y Cirugia Bucal 12(2):E134-138 [https://scielo.isciii.es/scielo.php?script=sci_arttext&pid=S1698-69462007000200011]

Liu W, Jin C-Z, Zhang Y-Q et al (2010) Human remains from Zhirendong, South China, and modern human emergence in East Asia. Proceedings of the National Academy of Sciences 107 (45):19201-19206 [https://doi.org/10.1073/pnas.1014386107]

Lucas PW, Constantino P, Wood B et al (2008) Dental enamel as a dietary indicator in mammals. BioEssays: news and reviews in molecular, cellular and developmental biology 30(4):374-385 [https://doi.org/10.1002/bies.20729]

Mallegni F, Trinkaus E (1997) A reconsideration of the Archi 1 Neandertal mandible. Journal of Human Evolution 33(6): 651-668 [https://doi.org/10.1006/jhev.1997.0159]

Mounier A, Heuzé Y, Samsel M et al (2020) Gravettian cranial morphology and human group affinities during the European Upper Palaeolithic. Scientific Reports 10(1):21931 [https://doi.org/10.1038/s41598-020-78841-x]

Olejniczak AJ, Smith TM, Feeney RN et al (2008) Dental tissue proportions and enamel thickness in Neandertal and modern human molars. Journal of Human Evolution 55(1):12-23 [https://doi.org/10.1016/j.jhevol.2007.11.004]

Posth C, Renaud G, Mittnik A et al (2016) Pleistocene Mitochondrial Genomes Suggest a Single Major Dispersal of Non-Africans and a Late Glacial Population Turnover in Europe. Current Biology 26(4):557-561 [https://doi.org/10.1016/j.cub.2016.02.022]

Potter RH, Nance WE, Yu P-L et al (1976) A twin study of dental dimension. II. Independent genetic determinants. American Journal of Physical Anthropology 44(3):397-412 [https://doi.org/10.1002/ajpa.1330440304]

Rajab LD, Hamdan MAM (2002) Supernumerary teeth: review of the literature and a survey of 152 cases. International Journal of Paediatric Dentistry 12(4):244-254 [https://doi.org/10.1046/j.1365-263X.2002.00366.x]

Rak Y, Kimbel WH, Hovers E (1994) A Neandertal infant from Amud Cave, Israel. Journal of Human Evolution 26(4):313-324 [https://doi.org/10.1006/jhev.1994.1019]

Rak Y, Kimbel WH, Hovers E (1996) On Neandertal autapomorphies discernible in Neandertal infants: a response to Creed-Mileset al. Journal of Human Evolution 30(2):155-158 [https://doi.org/10.1006/jhev.1996.0012]

Scheuer L, Black S (2000) Developmental juvenile osteology. Academic Press, London, 587 p

Schwartz GT (2000) Taxonomic and functional aspects of the patterning of enamel thickness distribution in extant large-bodied hominoids. American Journal of Physical Anthropology 111(2):211-244 [https://doi.org/10.1002/(SICI)1096-8644(200002)111:2<221::AID-AJPA8>3.0.CO;2-G]

Schwartz JH, Tattersall I (2000) The human chin revisited: what is it and who has it? Journal of Human Evolution 38(3):367-409 [https://doi.org/10.1006/jhev.1999.0339]

Shang H, Trinkaus E (2010) The early modern human from Tianyuan Cave, China. Texas A&M University Press, College Station, 272 p

Sikora M, Seguin-Orlando A, Sousa VC et al (2017) Ancient genomes show social and reproductive behavior of early Upper Paleolithic foragers. Science 358(6363):659-662 [https://doi.org/10.1126/science.aao1807]

Slon V, Mafessoni F, Vernot B et al (2018) The genome of the offspring of a Neanderthal mother and a Denisovan father. Nature 561(7721):113-116 [https://doi.org/10.1038/s41586-018-0455-x]

Spoor F, Zonneveld F, Macho GA (1993) Linear measurements of cortical bone and dental enamel by computed tomography: applications and problems. American Journal of Physical Anthropology 91(4):469-484 [https://doi.org/10.1002/ajpa.1330910405]

Teschler-Nicola M (2006) Early modern humans at the Moravian Gate: Mladec Caves and their remains, 1st ed edn. Springer, New York, 528 p

Trinkaus E (2002) The mandibular morphology In: Zilhao J, Trinkaus E (eds) Portrait of the Artist as a Child The Gravettian Human Skeleton from the Abrigo do Lagar Velho and its archaeological context Lisboa, pp 312-325

Trinkaus E (2007) European early modern humans and the fate of the Neandertals. Proceedings of the National Academy of Sciences 104(18):7367-7372 [https://doi.org/10.1073/pnas.0702214104]

Trinkaus E, Buzhilova AP, Mednikova MB et al (2014) The People of Sunghir: Burials, Bodies and Behavior in the Earlier Upper Paleolithic. Oxford University Press, New York, 339 p

Trinkaus E, Constantin S, Zilhão J (2012) Life and Death at the Pestera cu Oase: A Setting for Modern Human Emergence in Europe Oxford University Press, New York, 437 p

Trinkaus E, Moldovan O, Milota Ş et al (2003) An early modern human from the Peştera cu Oase, Romania. Proceedings of the National Academy of Sciences 100(20):11231-11236 [https://doi.org/10.1073/pnas.2035108100]

Verna C, Dujardin V, Trinkaus E (2012) The Early Aurignacian human remains from La Quina-Aval (France). Journal of Human Evolution 62(5):605-617 [https://doi.org/10.1016/j.jhevol.2012.02.001]

Villanea FA, Schraiber JG (2019) Multiple episodes of interbreeding between Neanderthal and modern humans. Nat Ecol Evol 3 (1):39-44 [https://doi.org/10.1038/s41559-018-0735-8]

Villotte S, Samsel M, Sparacello V (2017) The paleobiology of two adult skeletons from Baousso da Torre (Bausu da Ture) (Liguria, Italy): Implications for Gravettian lifestyle. Comptes Rendus Palévol 16(4):462-473 [https://doi.org/10.1016/j.crpv.2016.09.004]

Zilhão J, Trinkaus E (2002) Portrait of the artist as a child. The Gravettian human skeleton from the Abrigo do Lagar Velho and its archeological context, 1st ed edn. Instituto Português de Arqueologia, Lisboa, 609 p

The mandible and teeth characteristics of the Gravettian child from Gargas, France
Caractéristiques de la mandibule et des dents de l'enfant gravettien de Gargas, France

Supplementary Information

Mona Le Luyer[1*], Sébastien Villotte[2,3*], Priscilla Bayle[1], Selim Natahi[1], Adrien Thibeault[1], Bruno Dutailly[1,4], Carole Vercoutère[5], Catherine Ferrier[1], Christina San Juan-Foucher[6,7], Pascal Foucher[6,7]

1. Unité Mixte de Recherche 5199, de la Préhistoire à l'Actuel : Culture, Environnement et Anthropologie (PACEA), Centre National de la Recherche Scientifique (CNRS), Université de Bordeaux, Pessac, France
2. Unité Mixte de Recherche 7206 Eco-anthropologie, MNHN, CNRS, UP, Musée de l'Homme, Paris, France
3. Directorate Earth and History of Life, Royal Belgian Institute of Natural Sciences, Belgique
4. Unité Mixte de Service 3657, Archéovision, Centre National de la Recherche Scientifique (CNRS), Université Bordeaux-Montaigne, Pessac, France
5. Unité Mixte de Recherche 7194, Histoire Naturelle de l'Homme Préhistorique, Département Homme et Environnement, Centre National de la Recherche Scientifique (CNRS), Muséum national d'Histoire naturelle, Paris, France
6. Service régional de l'archéologie d'Occitanie, Toulouse, France
7. Unité Mixte de Recherche 5608, Travaux et Recherches Archéologiques sur les Cultures, les Espaces et les Sociétés (TRACES), Centre National de la Recherche Scientifique (CNRS), Université de Toulouse Jean Jaurès, Toulouse, France

* corresponding authors: mona.leluyer@outlook.com, sebastien.villotte@cnrs.fr

SI-1 The Gargas cave, the discovery and dating of the immature human mandible

The Gargas cave is located in the South-West of France (Fig. S1), in the village of Aventignan (43°03'20.2"N 0°32'09.4"E). Excavations at Gargas, famous for its parietal art (paintings and engravings) and especially the negative hands with incomplete fingers, have been carried out since the end of the XIXth century.

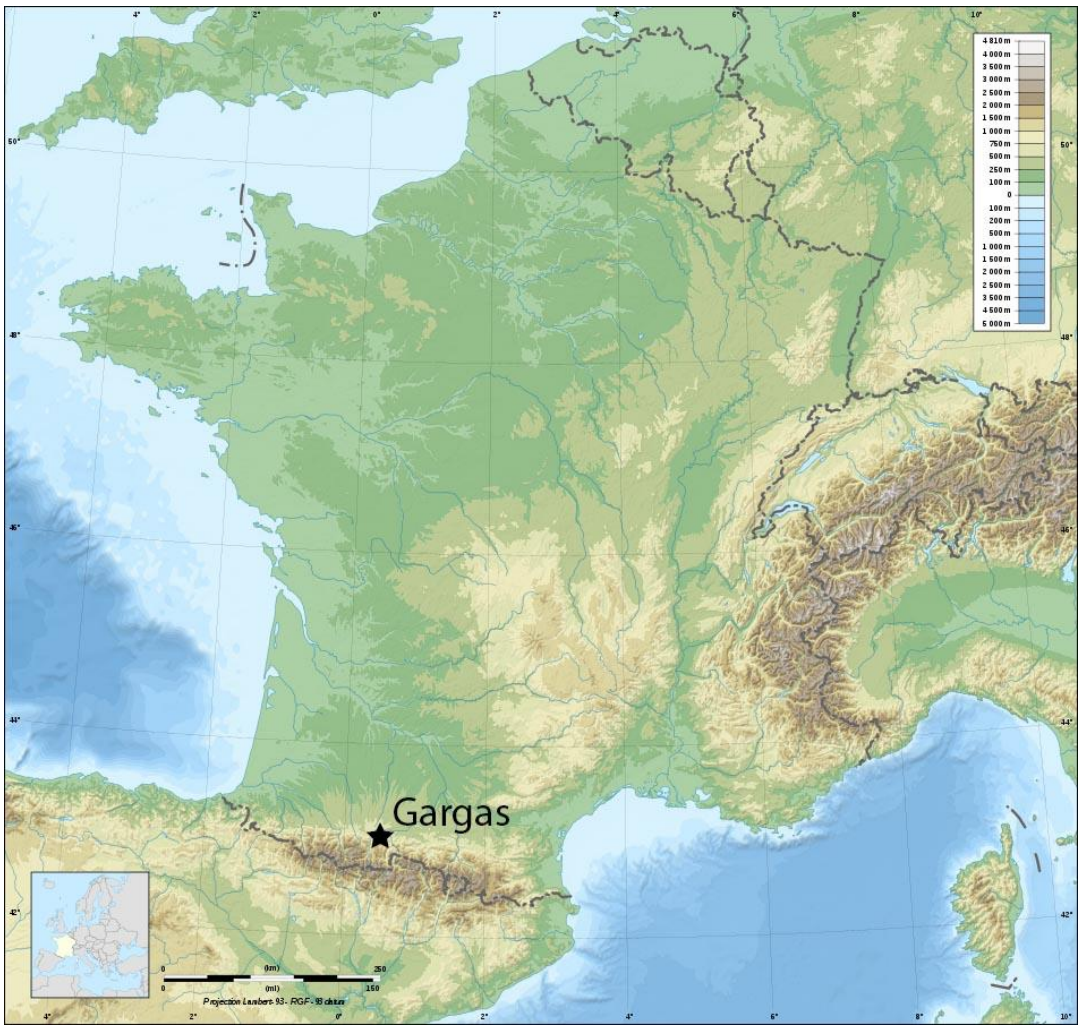

Figure S1. Map showing the location of the Gargas cave / *Carte montrant la localisation de la grotte de Gargas*

The human immature mandible was discovered in September 2011 in a new excavation sector (GPA) in the central zone of Room I, where two thirds of the painted hands are located (Foucher et al. 2012). This sector is at the foot of a large stalagmite prolonged into a stalagmite floor with a tilt of about 30°. Two fragments (GPA-646a and GPA-646b) of a human immature mandible were unearthed in layer 2 (at about 12 cm under the stalagmite floor) (Foucher et al. 2012). The two mandibular fragments were initially left *in situ* in order to conduct anthropological field observations. At that time, no clear sign of an intentional deposit or other indications of body treatment were found (Foucher et al. 2012). The mandible was then removed by Dominique Henry-Gambier (PACEA, University of Bordeaux) following an established protocol for DNA

research. Marie-France Deguilloux (PACEA, University of Bordeaux) sampled a small piece of bone from the lower portion of the right body of GPA-646b to attempt an extraction of endogenous DNA (Foucher et al. 2012). Unfortunately, this extraction failed (Deguilloux, pers. com.). A small portion of the inferior part of the body of GPA-646b was sampled for C14 direct dating. The radiocarbon date (Table S1) confirms the attribution to the Gravettian (Foucher et al. 2019) that was previously established only by depositional and archaeological context (Foucher et al. 2012).

Table S1. Direct dating of the mandible GPA-646 *Datation directe de la mandibule GPA-646*

Sample	**AMS BP**	**Lab reference**	**Date cal BP (1σ)**	**Date cal BP (2σ)**	**Reference**
GPA-646	24 930 ± 220	Ly-12478-SacA43642	29 224-28 726	29 500-28 532	Foucher et al. 2019

Calibration: OxCal v4.2.4 (Bronk Ramsey and Lee 2013), IntCal13 atmospheric curve (Reimer et al. 2013).

SI-2 The mandible GPA-646 and its teeth

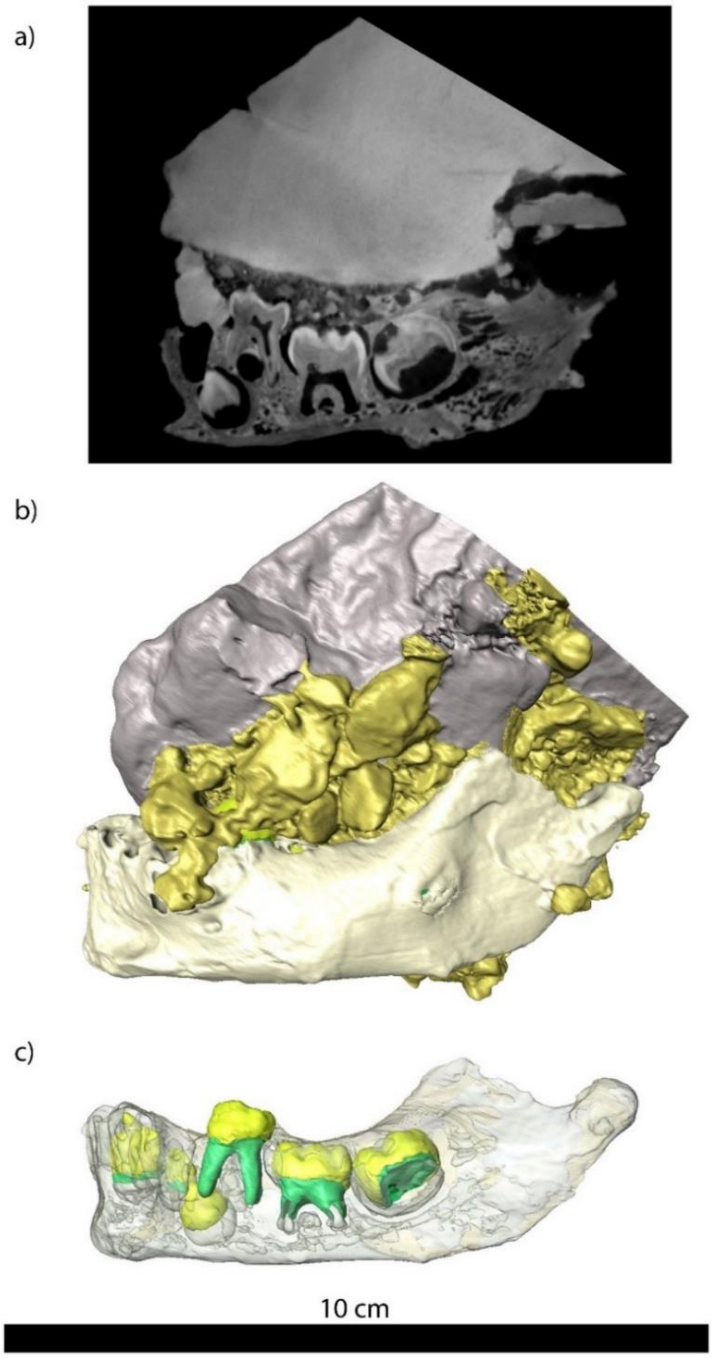

Figure S2. Left lateral view of GPA-646a. a) MicroCT-based virtual section passing approximately across its midportion. b) 3D rendering of the fossil fragment (shown in beige) attached to the flat triangular pebble (shown in grey) by a layer of concretion (shown in gold). c) 3D rendering of the bone (in semi-transparency) and the *in situ* teeth (the enamel is shown in yellow, dentine in green and bone in white) / *Vue latérale gauche de GPA-646. a) Section virtuelle passant approximativement à travers la portion médiane. b) Rendu 3D du fragment fossile (représenté en beige) attaché au galet triangulaire plat (représenté en gris) par une couche de concrétion (représenter en or). c) Rendu 3D de l'os (en semi-transparence) et des dents incluses (l'émail est représenté en jaune, la dentine en vert et l'os en blanc).*

Twelve teeth or germs are present (see Fig. 2): the four permanent incisors, a supernumerary tooth with a permanent incisor shape located on the right part of the anterior arcade, the two permanent canines, the LLdm1, the LRdm1, the LRP3, the LLP3, the LLdm2, and the LLM1. Three of these teeth (the LRdm1, the LRP3 and the LRC) are preserved in the fragment GPA-646b for which we obtained a higher resolution of microCT acquisition, whereas the others are preserved in the larger fragment GPA-646a.

Only the deciduous teeth were erupted at the time of death of the Gargas child. Deciduous incisors were likely fully erupted, whereas it seems less clear for the canines. The LLdm1 and LRdm1 were in full occlusion, as shown by slight wear facets on their metaconid and entoconid, with no dentine exposure (stage 1 according to Smith (1984)). The two roots of the Ldm1s embrace the margins of the crypts for the P3. The roots are developed to approximatively three quarters of the root length. Better observations can be done for the LRdm1, considering the higher resolution of the microCT record. The apex of the mesial root of the LRdm1 is more open than the apex of the distal one. The middle third of the mesial surface of the distal root and the distal third of the distal surface of the mesial root are lysed, very likely related to the development of the crypt for the P3. The pulp chamber of the LRdm1 displays four well-developed horns corresponding to each cusp. Only a single, large and flat canal is visible for each of the roots, the canal of the distal root being larger than the canal of the mesial one. These morphological characteristics seem similar for the LLdm1 but it is difficult to ascertain this considering the lower resolution for the fragment GPA-646a and the presence of concretion all around the roots and in the root canals.

The germs of five permanent incisors are lodged in their crypt in the alveolar bone of GPA-646a. The supplemental lateral incisor caused crowding in the anterior alveolar region. Four of the incisor germs are aligned in a traverse plan (their incisal edge lying *ca.* 2mm below the alveolar bone margin), whereas the fifth one is positioned slightly superiorly. The four aligned germs appear to have a similar stage of development: the enamel formation is complete at the occlusal surface and extends towards the cervical region (representing more or less three quarters of the final completed crown), and a dentinal deposit starts. The two LI1 germs measure *ca.* 6.0 mm high from the incisal edge to the farthest point on the base margin, whereas the two lateral LI2s measure *ca.* 5.0 mm. The fifth permanent incisor, located slightly above the two other right germs and called "supernumerary" (see Fig. 2b and Fig. S3a), appears less developed (even though it is difficult to be sure considering the lower resolution of the microscanner acquisition): the enamel extension may represent only half of the final completed crown. Its crown measures approximatively 4.7 mm from its incisal edge to the base margin. The supernumerary incisor is thus smaller than the LLI2 and LRI2 germs. However, in term of morphology of the enamel-dentine junction (EDJ), the LLI2 and the supernumerary incisor seem closer (Fig. S3b). The permanent LLC germ is located mesially to the mesial root of the LLdm1, whereas the LRC germ is at the level of the mesial rood of the LRdm1. Both germs lie low in the mandibular corpus, their tips being approximatively at the level of the dm1s root apexes. The buccal surface of the germ of the LRC is firmly attached by concretion to the distal wall of the crypt (presumably rotated postmortem). This crypt is open mesially at the anterior break of GPA-646b. Both germs measure *ca.* 6.2 mm high from cusp tip to crown base, which represent *ca.* half of the final complete crown height. The LLP3 germ is contained in its bony crypt. Its degree of maturation is very difficult to assess considering the presence of concretion within the crypt and the resolution of the microCT record. Only the buccal cusp of the LRP3 germ is formed (measuring *ca.* 2.1 mm from tip to base). This cusp is firmly attached by concretion to the distal part of the wall of it is crypt. The LLdm2 reaches the stage of alveolar eruption. The crown formation is complete. The radicular bifurcation is clearly visible with the mesial and distal roots formed to a length of approximatively 5.0 mm below the cervix. Below the LLdm2, the crypt for the LLP4 was forming at the time of death. The LLM1 germ lies in its crypt partly filled by

concretions. Its occlusal surface point in a mesiolingual direction. The height of the crown measured from the mesial cusps to the mesiobuccal cervix, is 5.8 mm, representing *ca.* three quarters of the final completed crown height. There is no defined pulp roof.

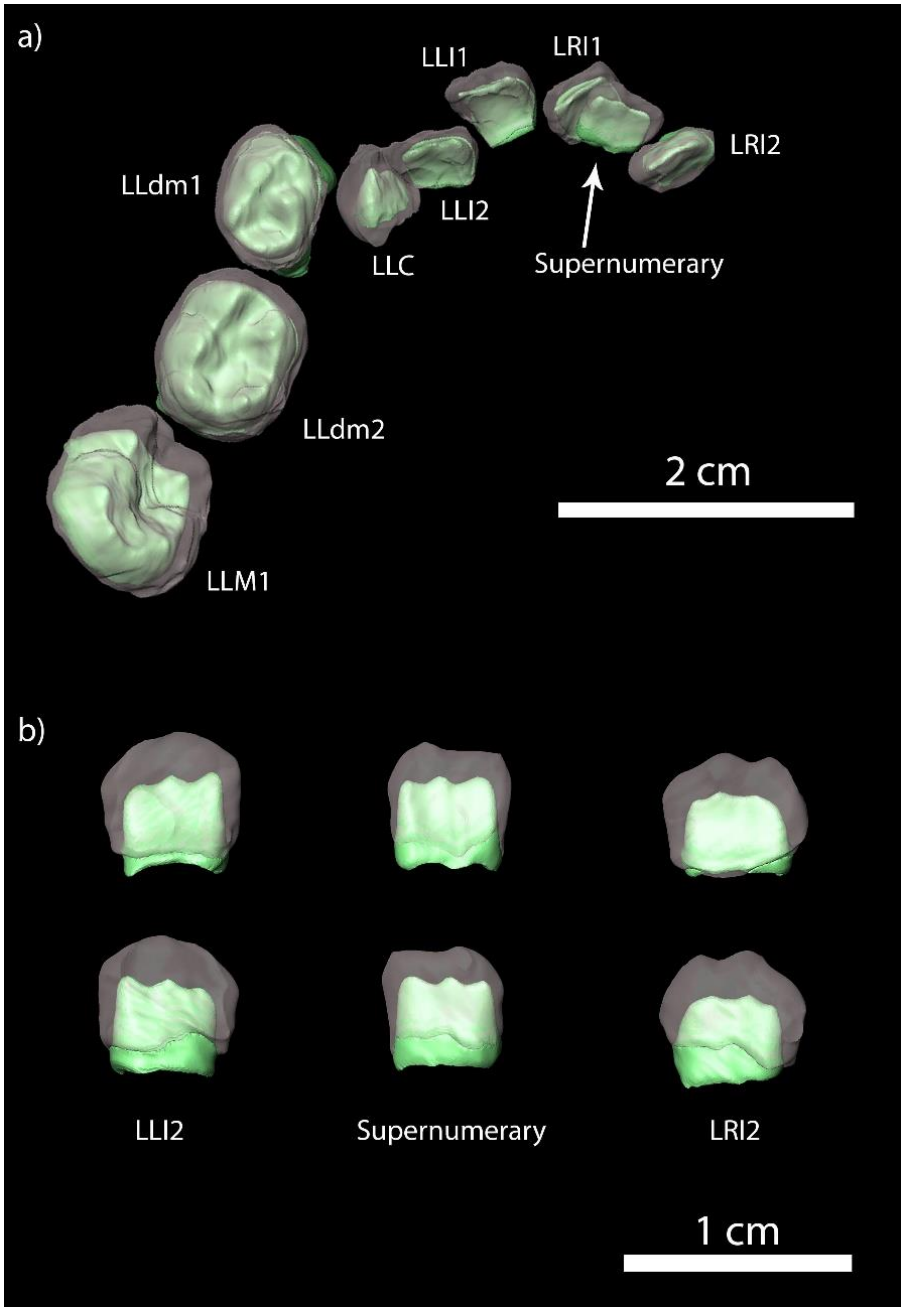

Figure S3. MicroCT-based 3D rendering of GPA-646a virtually extracted teeth and germs showing the enamel in semi-transparency and the dentine in green. a) positions of the teeth preserved *in situ* in the mandible with the deciduous molars in occlusal view. b) close-ups of the lingual (top) and buccal (bottom) views of the lateral incisors and the supernumerary tooth / *Rendu 3D des dents et des germes de GPA-646a extraits virtuellement montrant l'émail en semi-transparence et la dentine en vert. a) positions des dents préservées in situ dans la mandibule avec les molaires déciduales en vue occlusale. b) gros plans sur les incisives latérales et la dent surnuméraire en vues linguales (en haut) et buccales (en bas).*

Table S2. Reported cases of supernumerary teeth in Early and Mid-Upper Palaeolithic specimens / *Cas reportés de dents surnuméraires pour des spécimens du Paléolithique supérieur ancien et moyen*

Specimen ***(Age/sex)***	**Site**	**Technocomplex** ***Date***	**Description of the supernumerary tooth**
Pataud 1 *(young adult female)*	Abri Pataud, France	Final Gravettian *28,000–26,000 cal BP*	Two supernumerary teeth of simple conical form, adjacent to the URM2 and the URM1/URM2 (Legoux 1972, 1974, 1975 ; Villotte et al. 2018)
Dolní Věstonice 15 *(20-25 year-old male)*	Dolní Věstonice II, Czech Republic	Pavlovian *31,110–30,720 cal BP*	Unerupted mandibular supernumerary tooth of simple conical crown, adjacent to the left C and P3 roots (Hillson 2006 ; Trinkaus et al. 2006)
Dolní Věstonice 33	Dolní Věstonice II, Czech Republic	Pavlovian *~27,000–25,000 cal BP*	Small, unusual in morphology, unerupted isolated supernumerary tooth (Hillson 2006 ; Trinkaus et al. 2006)
Pavlov 21	Pavlov I, Czech Republic	Pavlovian *~27,000–25,000 cal BP*	Globular crown, fully erupted, isolated supernumerary tooth (Hillson 2006 ; Trinkaus et al. 2006)
Sunghir 2 *(~12 year-old male)*	Sungir, Russia	Sungirian *~35,280-33,180 cal BP*	Small, conical supernumerary tooth on the mesiolingual corner of the URI2 (Trinkaus 2018)

SI-3 Teeth development and Bayesian analysis

The Bayesian analysis of the dental maturational sequence of the Gargas child is based on a tooth-by-tooth evaluation of dental mineralization stages according to the scoring system (crown and root calcification) established by Demirjian et al. (1973) for the permanent teeth (Table S3). The estimation relies upon the microCT-based examination of the teeth preserved *in situ* within the mandible.

Table S3. Dental maturation of the GPA-646 mandible assessed following the scoring system of AlQahtani et al. (2010) for all the teeth and Demirjian et al. (1973) for the permanent teeth only / *Maturation dentaire de la mandibule GPA-646 évaluée selon les systèmes de cotation de AlQahtani et al. (2010) pour toutes les dents et Demirjian et al. (1973) pour les dents permanentes seules*

Tooth	**Developmental stage**	**Descriptive criteria of crown and root calcification**
LLi1		Lost postmortem, likely complete
LRi1		Lost postmortem, likely complete
LLi2		Lost postmortem, likely complete
LRi2		Lost postmortem, likely complete
LLc		Lost postmortem, complete?
LRc		Lost postmortem, complete?
LLm1	Rc	Crown formation complete, root length complete with parallel ends
LRm1	R 3/4	Crown formation complete, three quarters of root length developed
LLm2	R 1/2	Crown formation complete, root length equals crown length
LLI1	Cr 3/4; C	Enamel formation complete at the occlusal surface, with extension towards the cervical region (crown three quarters completed) and initiation of dentine formation
LRI1	Cr 3/4; C	Enamel formation complete at the occlusal surface, with extension towards the cervical region (crown three quarters completed) and initiation of dentine formation
LLI2	Cr 3/4; C	Enamel formation complete at the occlusal surface, with extension towards the cervical region (crown three quarters completed) and initiation of dentine formation
LRI2	Cr 3/4; C	Enamel formation complete at the occlusal surface, with extension towards the cervical region (crown three quarters completed) and initiation of dentine formation
Supernumerary	Cr 3/4; C	Enamel formation complete at the occlusal surface, with extension towards the cervical region (crown three quarters completed) and initiation of dentine formation
LLC	Cr 1/2; C	Enamel formation complete at the occlusal surface, with extension towards the cervical region (crown half completed) and initiation of dentine formation
LRC	Cr 1/2; C	Enamel formation complete at the occlusal surface, with extension towards the cervical region (crown half completed) and initiation of dentine formation
LLP3	ci; A	Beginning of calcification at the superior level of the crypt in the form of an inverted cone
LRP3	Cco; A	Beginning of calcification at the superior level of the crypt in the form of an inverted cone

LLP4	/; 0	No initiation
LRP4	/; 0	No initiation
LLM1	Cr 3/4; C	Enamel formation complete at the occlusal surface, with extension towards the cervical region and initiation of dentine formation
LLM2	/; 0	No initiation

The sequence composed by the permanent teeth was compared to those assessed following the same scoring method on a radiographic and CT reference sample of 795 living humans (408 females and 387 males) of African, European and Middle Eastern origins, aged 1-8 years and distributed as follows: 1-2 years = 14 individuals; 2-3 = 21; 3-4 = 74; 4-5 = 119; 5-6 = 153; 6-7 = 178; 7-8 = 236. The statistical analysis of each dental mineralization sequence was realized by applying the approach developed by Braga and Heuzé (2007), using Bayes's rule of conditional probability (Vieland 1998 ; Aitken and Taroni 2004), with teeth being considered as statistically dependent units and prior probabilities uniform. The results of the Bayesian analysis of the mineralization sequence (C/C/C/A/0/C/0) displayed by the permanent teeth (I1/I2/C/P3/P4/M1/M2) are presented in Table S4.

Table S4. Results of the Bayesian analysis run for the permanent mineralization sequence of GPA-646 / *Résultats de l'analyse bayésienne de la séquence de minéralisation permanente de GPA-646*

Specimen (sequence)	**GPA-646 (C/C/C/A/0/C/0)**
N individuals in comparative sample	795
N theoretical combinations	126
N calculated combinations	126 (100%)
N sequences cf. Gargas child	1
$p<0.25$	0
Probability balance (%) $0.25 \leq p \leq 0.75$	0
$p>0.75$	100

Within the comparative sample of 795 extant children aged 1-8 years used in this study, the mineralization sequence displayed by the mandible GPA-646 occurs only once. All the posterior probabilities associated with the observed combinations (n = 126) have been efficiently calculated and all are higher than 0.75. Although 0.75 does not represent an absolute cutoff in a continuous probability distribution (ranging from 0 to 1), probabilities higher than this formal threshold indicate very likely events, whereas values between 0.25 and 0.75 are more likely to be associated with random events, and values lower than 0.25 with unlikely events (Braga and Heuzé 2007).

In summary, according to the present Bayesian analysis, the occurrence of a mineralization sequence like the one found in the Gargas child is common in extant humans of African, European, and Middle Eastern origins. In the comparative record specifically used in this study, the extant child that shares a mineralization sequence with the Gravettian fossil is a girl aged 1.48 years.

SI-4 Methodology for virtual measurements

For the mandibular dimensions, 26 measurements were taken on the 3D models using Avizo, Fiji, and TIVMI (Treatment and Increased Vision for Medical Imaging) software. Using 3D landmarks or 2D slide extractions, virtual measurements were repeated three times at least one week apart. Results are provided in Table S5. Differences between repeated measurements were negligible (all CV<5%, 19 being under 2%), the values obtained for each measurement were averaged and used to describe the mandibular dimensions in this study.

In order to measure the mesiodistal and buccolingual crown diameters of the posterior teeth, a specific protocol was created using TIVMI. First, a path3D is created by placing a large set of points around the cervix of the tooth at regular intervals. The best-fit plane at the cervix is computed from this path3D. Two points are thus defined: the most mesial and the most distal one. The mesiodistal plan is created as the plane orthogonal to the cervix plane and passing through these two points. The buccolingual plane, orthogonal to the two other ones, is then generated. The two points of the mesh of the crown that are the most distant from the buccolingual plane are identified using the plugin "bench vice". The distances between each point and the vestibulolingual plane are summed up in order to compute the mesiodistal diameter. The same approach is applied for the vestibulolingual diameter. The early maturational stage for the anterior teeth prevents the application of the same protocol. The mesiodistal diameter was directly computed with TIVMI as the distance between the most mesial and most distal points of the crown. The computed mesiodistal diameters for the anterior teeth are thus considered as approximations.

For describing 3D tissue proportions and enamel thickness, seven linear, surface, and volumetric variables were digitally measured from the crown of the LRdm1 using Avizo 7.1 or calculated: the volume of the crown (mm^3), the volume of the enamel cap (mm^3), the volume of the dentine and pulp (mm^3), the percentage of the crown volume that is dentine and pulp (%), the surface area of the EDJ (mm^2), the average enamel thickness (3D AET, mm), and the scale-free relative enamel thickness (3D RET) (Martin 1985 ; Olejniczak et al. 2008). Two-dimensional dental tissue proportions and enamel thickness were measured on a virtual buccolingual cross-section through the two mesial dentine horn tips(Martin 1985 ; Olejniczak et al. 2008). Seven linear and surface variables were measured from this buccolingual cross-section using MPSAK v. 2.9 (available in Dean and Wood (2003)) or calculated: the crown area (mm^2), the enamel area (mm^2), the dentine and pulp area (mm^2), the percentage of the crown area that is dentine and pulp (%), the EDJ length (mm), the 2D AET (mm), and the 2D RET. All comparative teeth used for dental tissue proportions and enamel thickness analysis show an occlusal wear stage from 1 (unworn to polished or small facets) to 3 (small dentine exposure) according the scoring system of Smith (Smith 1984). For slightly worn crowns, corrections of outer enamel surface were made prior to measurements of 2D variables. Reconstructions of the removed enamel were performed based on the morphology observed for unworn teeth in virtual buccolingual cross-sections (Smith et al. 2012).

Table S5. Results of the virtual measurements for the mandible, repeating three times (#1, #2 and #3) using landmarks (L) and slide extractions (S). sd=standard deviation, CV=coefficient of variation / *Résultats des mesures virtuelles de la mandibule*, prises à trois répétitions *(#1, #2 et #3) en utilisant les landmarks (L) et les sections virtuellement extraites (S). sd=déviation standard, CV=coefficient de variation*

M#	Measurements	Method	#1	#2	#3	Mean	*sd*	CV
67	Bimental breadth	L	35.10	35.02	35.03	**35.05**	*0.04*	0.12%
	Bi-external dc arcade breadth	L	32.10	32.10	32.04	**32.08**	*0.03*	0.11%
	Bi-external dm1 arcade breadth	L	40.68	40.75	40.84	**40.76**	*0.08*	0.20%
69	Symphyseal height	S	19.79	20.1	20.28	**20.06**	*0.25*	1.24%
	Symphyseal breadth	S	10.40	10.42	10.33	**10.38**	*0.05*	0.46%
	Ldi1-Ldi2 height	S	20.87	21.00	21.06	**20.98**	*0.10*	0.46%
	Ldi1-Ldi2 breadth	S	10.71	10.3	10.55	**10.52**	*0.21*	1.96%
	Ldi2-Ldc height	S	18.37	18.19	18.46	**18.34**	*0.14*	0.75%
	Ldi2-Ldc breadth	S	10.54	10.43	10.90	**10.62**	*0.25*	2.31%
	Ldc-Ldm1 height	S	18.09	17.90	17.95	**17.98**	*0.10*	0.55%
	Ldc-Ldm1 breadth	S	10.32	10.62	10.47	**10.47**	*0.15*	1.43%
	Ldm1-Ldm2 height	S	16.24	16.56	15.96	**16.25**	*0.30*	1.84%
	Ldm1-Ldm2 breadth	S	11.76	11.87	12.03	**11.89**	*0.13*	1.13%
69(1)	Height at the left mental foramen	S	18.28	17.41	17.30	**17.66**	*0.54*	3.04%
69(3)	Breadth at the left mental foramen	S	9.66	10.43	10.47	**10.19**	*0.46*	4.48%
	Rdi1-Rdi2 height	S	20.52	20.65	20.52	**20.56**	*0.08*	0.36%
	Rdi1-Rdi2 breadth	S	10.99	10.54	11.24	**10.92**	*0.35*	3.25%
	Rdi2-Rdc height	L	18.87	18.10	-	**18.48**	*0.55*	2.95%
	Rdi2-Rdc height	S	19.15	19.26	18.40	**18.94**	*0.47*	2.47%
	Rdi2-Rdc breadth	S	10.24	10.91	10.55	**10.57**	*0.34*	3.17%
	Rdc-Rdm1 height	S	17.92	18.02	18.00	**17.98**	*0.05*	0.29%
	Rdc-Rdm1 breadth	S	11.98	11.3	11.17	**11.48**	*0.44*	3.79%
	Rdm1-Rdm2 height	S	17.49	18.82	17.98	**18.10**	*0.67*	3.72%
	Rdm1-Rdm2 breadth	S	11.31	10.43	10.95	**10.90**	*0.45*	4.08%
69(1)	Height at the right mental foramen	S	17.90	18.07	17.70	**17.89**	*0.19*	1.04%
69(3)	Breadth at the right mental foramen	S	10.80	10.51	10.40	**10.57**	*0.21*	1.95%

SI-5 Comparative samples for metric analyses

Mandibular measurements of GPA-646 were compared with those of 90 immature specimens (Table S6): 23 Neandertals, 29 Upper Palaeolithic modern humans and 38 modern humans from osteological collections. Each specimen is attributed to an age class (S1, S2, S3 or S4) based on dental eruption according to Verna et al. (2012).

Dental crown dimensions of GPA-646 permanent and deciduous teeth were compared with mesiodistal and buccolingual dimensions of a minimum number of 107 Neandertals, 150 Upper Palaeolithic and 60 Holocene modern humans (Table S7). The total comparative samples include 111 LI1s, 147 LI2s, 148 LCs, 235 LM1s, 85 Ldm1s, 105 Ldm2s.

Dental tissue proportions and enamel thickness of the LRdm1 of GPA-646 were compared to those of 7 Neandertals, 14 Upper Palaeolithic modern humans and 6 Holocene modern humans (Table S8).

Table S6. Comparative samples for the mandibular corpus dimensions / *Échantillons de comparaison pour les dimensions du corps mandibulaire*

Group	Specimen	Country	Age	Age class	Reference
Neandertal	Chaise 13	France	4.5	S1	Tillier and Genet-Varcin (1980)
	Chateauneuf-sur-Charente	France	3	S1	Patte (1957)
	Combe Grenal 1	France	6.5	S2	Garralda and Vandermeersch (2000)
	Hortus 2	France	9.5	S3	De Lumley (1973)
	Malarnaud 1	France	12	S4	Trinkaus, pers. data
	Pech-de-l'Azé	France	2.5	S1	Ferembach (1969), Ferembach et al. (1970), Trinkaus, pers. data
	Petit-Puymoyen 1	France	13	S4	Trinkaus, pers. data
	Roc-de-Marsal 1	France	2.75	S1	Madre-Dupouy (1992)
	Devil's Tower 2	Gibraltar	3.75	S1	Tillier (1982), Dean et al. (1986)
	Archi 1	Italy	3	S1	Mallegni and Trinkaus (1997b)
	Fate 2	Italy	9.5	S3	de Lumley and Giacobini (2013a)
	Molare 1	Italy	3.5	S1	Mallegni and Ronchitelli (1987)
	Amud 7	Israel	0.75	S0	Rak et al. (1994)
	Barakai 1	Russia	3	S1	Faerman et al. (1994)
	Zaskalnaya VI	Russia	10.5	S3	Kolosov et al. (1974)
	Cova Negra 7755	Spain	6	S2	Arsuaga et al. (1989)
	Palomas 7	Spain	4	S1	Walker et al. (2010)
	Palomas 49	Spain	2	S1	Walker et al. (2010)
	Palomas 80	Spain	11	S3	Walker et al. (2010)
	Dederiyeh 1	Syria	1.95	S1	Akazawa and Muhesen (2003)

	Dederiyeh 2	Syria	2.15	S1	Akazawa and Muhesen (2003)
	Teshik-Tash 1	Uzbekistan	10	S3	Gremyatskij (1949), Tillier (1979b)
	Šipka 1	Czech Republic	8.5	S3	Minugh-Purvis (2000)
Early Upper Palaeolithic modern humans	QuinaA 4	France	5.5	S2	Verna et al. (2012)
	Les Rois A-aver	France	11	S3	Trinkaus, pers. data
	Ksar Akil 1	Lebanon	8	S2	Bergman and Stringer (1989)
Mid Uppper Palaeolithic modern humans	Miesslingtal 1	Austria	5.5	S2	Trinkaus, pers. data
	Předmostí 2	Czech Republic	7	S3	Hrdlička (1924)
	Předmostí 24	Czech Republic	7.5	S3	Hrdlička (1924)
	Předmostí 25	Czech Republic	10	S3	Hrdlička (1924)
	Le Figuier 1	France	3	S1	Billy (1980)
	Paglicci 12	Italy	13.5	S4	Mallegni and Parenti (1972-1973)
	Caldeirão 2	Portugal	11	S3	Trinkaus et al. (2001)
	Lagar Velho 1	Portugal	4.75	S1	Zilhão and Trinkaus (2002)
	Kostenki 3	Russia	5	S1	Trinkaus, pers. data
	Kostenki 4	Russia	11	S3	Trinkaus, pers. data
	Sunghir 2	Russia	12	S4	Trinkaus et al. (2014)
	Sunghir 3	Russia	10	S3	Trinkaus et al. (2014)
	El Castillo C	Spain	4.5	S1	Garralda et al. (2019)
Late Upper Palaeolithic modern humans	Badegoule	France	3	S1	Trinkaus, pers. data
	Isturitz 119	France	4	S1	Trinkaus, pers. data
	Isturitz 64	France	6	S1	Trinkaus, pers. data
	Isturitz 65	France	1	S1	Trinkaus, pers. data
	Isturitz 68	France	7	S2	Trinkaus, pers. data
	Les Hoteaux 2	France	12	S4	Vallois (1972)
	Roc-de-Cave 1	France	15	S4	Bresson (2000)
	Saint Germain La Rivière 117	France	5.5	S2	Trinkaus, pers. data
	Saint Germain La Rivière 5	France	7	S3	Trinkaus, pers. data
	Saint Germain La Rivière 93	France	7	S3	Trinkaus, pers. data
	Arene candide 5B	Italy	3	S1	Trinkaus, pers. data
	Grotte des Enfants 1	Italy	3	S1	Henry-Gambier (2001)
	Grotte des Enfants 2	Italy	1.5	S1	Henry-Gambier (2001)
Holocene modern humans	Osteological collections, n=30	Italy and France	0 to 10.5	S1 to S3	Madre-Dupouy (1992), Mallegni and Trinkaus (1997b), Trinkaus, pers. data

S0 = no tooth erupted; S1 = deciduous dentition only; S2 = deciduous dentition and M1 fully erupted;
S3 = mixed dentition with the M1 and at least another permanent tooth fully erupted (but usually not the M2);
S4 = all permanent teeth fully erupted except the M3.

Table S7. Comparative samples for the dental crown dimensions / *Échantillons de comparaison pour les dimensions des couronnes dentaires*

Group	Site	Country	Specimen labels	References
Neandertal - Europe	Engis	Belgium	2	Tillier (1983)
	Spy	Belgium	1, 2	Trinkaus, pers. data
	Zaskalnaya	Crimea	VI	Kolossov et al. (1975)
	Vindija	Croatia	201, 206, 226, 231	Voisin et al. (2012)
	Kůlna	Czech Republic	4, 5	Trinkaus, pers. data
	Šipka	Czech Republic	1	Vlček (1969)
	Švédův stůl	Czech Republic	1	Trinkaus, pers. data
	Abri des Merveilles	France	1	Trinkaus (1976)
	Arcy-Hyène	France	8	Trinkaus, pers. data
	Arcy-Renne	France	7, 11, 18, 25, 29, 33, 35	Leroi-Gourhan (1958), Bailey and Hublin (2006)
	Caminero	France	D, E, G, I	Trinkaus, pers. data
	Châteauneuf-sur-Charente	France	1, 2	Patte (1957), Tillier (1979a)
	Combe-Grenal	France	1, 4	Garralda and Vandermeersch (2000)
	Genay	France	1, 3	De Lumley (1987), Garralda et al. (2008)
	Grotte de la Balauzière	France	no N°	Trinkaus, pers. data
	Hortus	France	2, 4, 5	De Lumley (1973)
	La Ferrassie	France	4b, 8	Heim (1982), Gómez-Olivencia et al. (2015)
	Le Moustier	France	1	Weinert (1925), Petit-Maire et al. (1971)
	Le Placard	France	no N°	Brabant and Twiesselmann (1964)
	Le Portel	France	1	Petit-Maire et al. (1971)
	Les Peyrards	France	2, 3	De Lumley (1973)
	Malarnaud	France	1	Trinkaus, pers. data
	Marillac	France	G	Trinkaus, pers. data
	Monsempron	France	1	Trinkaus, pers. data
	Montgaudier	France	5	Duport and Vandermeersch (1976)
	Pech de l'Azé	France	1	Ferembach et al. (1970)
	Petit-Puymoyen	France	1, 3, 4a	Trinkaus, pers. data
	Quina	France	5, 9, 21, 31	Verna (2006)
	Regourdou	France	1	Trinkaus, pers. data
	Roc de Marsal	France	1	Madre-Dupouy (1992)
	Saint Césaire	France	1	Vandermeersch (1984)
	Taubach	Germany	1, 2	Gieseler (1971)

	Devil's Tower	Gibraltar	2	Tillier (1982)
	Subalyuk	Hungary	1	Pap et al. (1996)
	Archi	Italy	1	Mallegni and Trinkaus (1997a), Trinkaus, pers. data
	Breuil	Italy	2	Manzi and Passarello (1995)
	Cavallo	Italy	A	Palma di Cesnola and Messeri (1967)
	Fate	Italy	2	de Lumley and Giacobini (2013b)
	Fossellone	Italy	3	Mallegni and Naldini-Segre (1992)
	Guattari	Italy	3	Mallegni (1995)
	Taddeo	Italy	1	Benazzi et al. (2011)
	Columbeira	Portugal	1	Trinkaus, pers. data
	Salemas	Portugal	1	Trinkaus, pers. data
	Agut	Spain	1	De Lumley (1973)
	Banolas	Spain	no N°	De Lumley (1973)
	Cova Negra	Spain	7755	Arsuaga et al. (2007)
	Sima de las Palomas	Spain	1, 18, 25, 26, 40, 50, 54, 59, 61, 70, 82, 83, 84, 88, 89	Pinilla and Trinkaus (2017)
	Valdegoba	Spain	1, 2	Quam et al. (2001)
	Zafarraya	Spain	1	García Sánchez (1987)
Neandertal - SW Asia	Shanidar	Iraq	2, 4, 6, 7	Trinkaus (1983)
	Amud	Israel	1, 3	Sakura (1970)
	Kebara	Israel	1, 2, 4, 28, 31	Tillier et al. (2003), Trinkaus, pers. data
	Tabun	Israel	1, B4	Trinkaus, pers. data
	Dederiyeh	Syria	1, 2	Mizoguchi (2002), Kondo and Ishida (2003)
	Teshik-Tash	Uzbekistan	1	Gremyatskij and Nesturkh (1949)
Early Upper Palaeolithic modern humans	Bacho Kiro	Bulgaria	1124	Glen and Kaczanowski (1982)
	Vindija	Croatia	286, 288	Voisin et al. (2012)
	Mladeč	Czech Republic	52, 54	Frayer et al. (2006)
	Nazlet Khater	Egypt	2	Crevecoeur (2008)
	Brassempouy	France	69, 112	Henry-Gambier et al. (2004)
	Font de Gaume	France	1, 2	Gambier et al. (1990)
	Fontéchevade	France		Henry-Gambier et al. (2004)
	Les Abeilles	France	2	Gambier (1992)
	La Quina Aval	France	1, 4	Verna et al. (2012)
	Les Rois	France	A, B, 50.24, R50, R50-33, R51-14, R51-16, A3-10, 31	Henry-Gambier et al. (2004), Trinkaus, pers. data
	Les Vachons	France	1	Frayer (1978)
	Peştera Muierii	Romania	1	Dobos et al. (2010)
	Oase	Romania	1	Trinkaus et al. (2003)

	Kostenki	Russia	9	Trinkaus, pers. data
	Sunghir	Russia	2, 3	Trinkaus et al. (2014)
	Castillo	Spain	2	Garralda et al. (1992)
Mid Upper Palaeolithic modern humans	Grub/Kranawetberg	Austria	1	Teschler-Nicola et al. (2004)
	Miesslingtal	Austria	22034	Trinkaus, pers. data
	Dolní Věstonice	Czech Republic	3, 13, 14, 15, 36	Trinkaus and Svoboda (2006)
	Pavlov	Czech Republic	1, 2, 7, 8, 9, 10, 25, 30, 32	Sladek et al. (2000), Hillson (2006)
	Předmostí	Czech Republic	1, 2, 3, 4, 5, 7, 9, 10, 14, 18, 26	Hrdlička (1924)
	Baousso da Torre	France	2	Villotte et al. (2017)
	Badegoule	France	1	Patte (1976), Trinkaus, pers. data
	Cro-Magnon	France	4	Villotte, pers. data
	Cuzoul de Vers	France		Henry-Gambier and Villotte (2012)
	Lachaud	France	1, 3, 5	Ferembach (1957)
	Le Figuier	France	1	Billy (1980)
	Le Placard	France	1	Trinkaus, pers. data
	Pataud	France	1, 2, 4, 8, 9	Legoux (1972), Villotte et al. (2015), Villotte, pers. data
	Pech de la Boissière	France	1	Gambier (1992)
	Arene Candide	Italy	1	Sergi et al. (1974)
	Barma Grande	Italy	2, 4, 5	Formicola (1988), Voisin et al. (2012)
	Grotte des Enfants	Italy	6	Sergi et al. (1974)
	Paglicci	Italy	12, 14, 17, 18, 24, 25, 33, 37	Mallegni and Parenti (1972-1973), Mallegni and Palma di Cesnola (1994)
	Caldeirão	Portugal	2, 5, 6, 11	Trinkaus et al. (2001)
	Lagar Velho	Portugal	1	Zilhão and Trinkaus (2002)
	Kostenki	Russia	3, 4	Trinkaus, pers. data
	Silická Brezová	Slovakia	1	Frayer (1978)
Late Upper Palaeolithic modern humans	Bruniquel	France	537, 538, 540	Trinkaus, pers. data
	Cap Blanc	France	1	Voisin et al. (2012)
	Isturitz	France	64, 65, 67, 81, 85, 86, 89, 106, 116, 118, 119, 2000	Gambier (1990-91)
	Lafaye	France	24, 25	Genet-Varcin and Miquel (1967), Le Luyer (2016), Le Roy and Henry-Gambier (2017)
	La Madeleine	France	1, 4	Frayer (1978), Heim (1991)
	Le Morin	France	A3, A4	Gambier and Lenoir (1991), Le Luyer (2016)
	Le Peyrat	France	5	Patte (1968)
	Les Hoteaux	France	1	Vallois (1972)

	Pont d'Ambon	France	P3, PA2	Gambier (1994)
	Roc-de-Cave	France	1	Bresson (2000)
	Saint Germain La Rivière	France	4, B41970.8, B31970.8	Blanchard et al. (1972); Voisin et al. (2012)
	Oberkassel	Germany	1, 2	Lacy (2015)
	Arene Candide	Italy	1, 2, 4, 5, 6, 8	Formicola (1986), Henry-Gambier (2001)
	Grotte des Enfants	Italy	1, 2	Henry-Gambier (2001)
	Romanelli	Italy	7, 22, 23, 24	Fabbri (1987)
	Romito	Italy	1, 2, 3, 4, 6	Fabbri and Mallegni (1988)
	Vado all' Arancio	Italy	1, 2	Henry-Gambier (2001), Minellono et al. (1980)
	Cisterna	Portugal	3	Trinkaus et al. (2011)
	El Mirón	Spain	1	Carretero et al. (2015)
	Aveline's hole	UK	9, 504, 506	Voisin et al. (2012)
	Badger Hole	UK	2	Trinkaus, pers. data
Holocene modern humans	Combe Capelle	France	1	Frayer (1978)
	Culoz-sous-Balme	France	2	Frayer (1978)
	Poeymaü	France	1	Vallois and de Felice (1977)
	Cheix	France	1	Verdène (1975)
	Cuzoul de Gramat	France	1	Verdène (1975)
	Les Fieux	France	D1, D2	(2016)
	Hoëdic	France	1, 3, 4, 6, 7, 8, 9, 10	Verdène (1975), Caillard (1976), Frayer (1978)
	Houleau	France	37, 97	Le Luyer (2016)
	La Vergne	France	7-1, 10-1	Le Luyer (2016)
	Les Perrats	France	3221	Le Luyer (2016)
	Auneau	France	3, 7	Le Luyer (2016)
	Téviec	France	1, 2, 3, 4, 9, 10, 11, 13, 14, 15, 16	Verdène (1975), Caillard (1976), Frayer (1978), Le Luyer (2016)
	Baume Bourbon	France	A, B, C, 2, 4, 5	Le Luyer (2016)
	Aven des Bréguières	France		Le Luyer (2016)
	Germignac	France	1	Le Luyer (2016)
	Pendimoun	France	F1, F2	Le Luyer (2016)
	Gurgy Les Noisats	France	201, 206, 215A, 215B, 243B, 258, 277	Le Luyer (2016)
	Grotte mykolas	France	9, 10, 12	Le Luyer (2016)
	Auneau	France	1, 2, 4, 5	Le Luyer (2016)6
	Baume de Montclus	France	1	Vallois and de Felice (1977)
	Rastel	France	1	Frayer (1978)
	Veyrier	France	3	Frayer (1978)

Table S8. Comparative samples for the dental tissue proportions and enamel thickness / *Échantillons de comparaison pour les proportions des tissus dentaires et l'épaisseur de l'émail*

Group	Site	Country	Specimen labels	References
Neandertal	La Chaise Abri Suard	France	S14-1a, S14-4, S37, S44	Bayle (2008)
	Roc de Marsal	France	1	Bayle et al. (2009b)
	Devil's Tower	Gibraltar	2	Bayle, pers. data
	Sima de las Palomas	Spain	25	Bayle et al. (2017)
Late Upper Palaeolithic modern humans	Lafaye	France	25	Le Luyer (2016)
	La Madeleine	France	4	Bayle et al. (2009a)
	La Marche	France	1, 3	Le Luyer (2016)
Holocene modern humans	Houleau	France	R17	Le Luyer (2016)
	La Vergne	France	10	Le Luyer (2016)
	Les Perrats	France	3221	Le Luyer (2016)
	Baume Bourbon	France	C	Le Luyer (2016)
	Gurgy Les Noisats	France	206, 244,258	Le Luyer (2016)
	Auneau Parc du Château	France	D128	Le Luyer (2016)
	Usseau	France	U21, U56, U57, U63	Bayle (2008)
	Osteological collections of the University of Poitiers and the Institut d'Anatomie de Strasbourg	France	Sbg1, Sbg2, UTP	Bayle (2008)

SI-6 Mandibular dimensions

Table S9. Osteometrics of the mandible GPA-646 / *Ostéométrie de la mandibule GPA-646*

M N°	Measurements	Left	Right
68(1)	Maximal projection mandibular length	77.5	
68	Length of the body	[58.2]	
66	Bigonial breadth*	[67.0]	
67	Bimental breath**	35.1	
	Bi-external dc arcade breadth**	32.1	
	Bi-external dm1 arcade breadth**	40.8	
70	Gonion-Condyle height	[33.0]	
70a	Projected length of the ramus	23.9	
70(2)	Minimum ramus height	[28.0]	
71	Width of the ramus	[28]	
71a	Minimum ramus antero-posterior width	26.5	
	Antero-posterior length of the condyle	8.0	
71(1)	Sigmoid notch breadth	(20.0)	
69	Symphysis height**	20.1	
	Symphysis breadth**	10.4	
69(1)	Height at the mental foramen**	17.7	17.9
69(3)	Breadth at the mental foramen**	10.2	10.6
	di1-di2 height**	21.0	20.6
	di2-dc height**	18.3	18.5
	dc-dm1 height**	18.0	18.0
	dm1-dm2 height**	16.3	18.1
	dm1-dm2 breadth**	11.9	10.9
79	Gonial angle	[150°]	
79c	Mental angle	[85°]	

All dimensions are in millimeters unless otherwise specified. M indicates measurement following the Martin system [20]. "(##)" indicates a measurement with small degree of estimation. "[##]" indicates a measurement with greater degree of estimation. *: Twice the distance from the midline (assessed from the symphyseal morphology) to the left side. **: Measured on the 3D models (see SI-5).

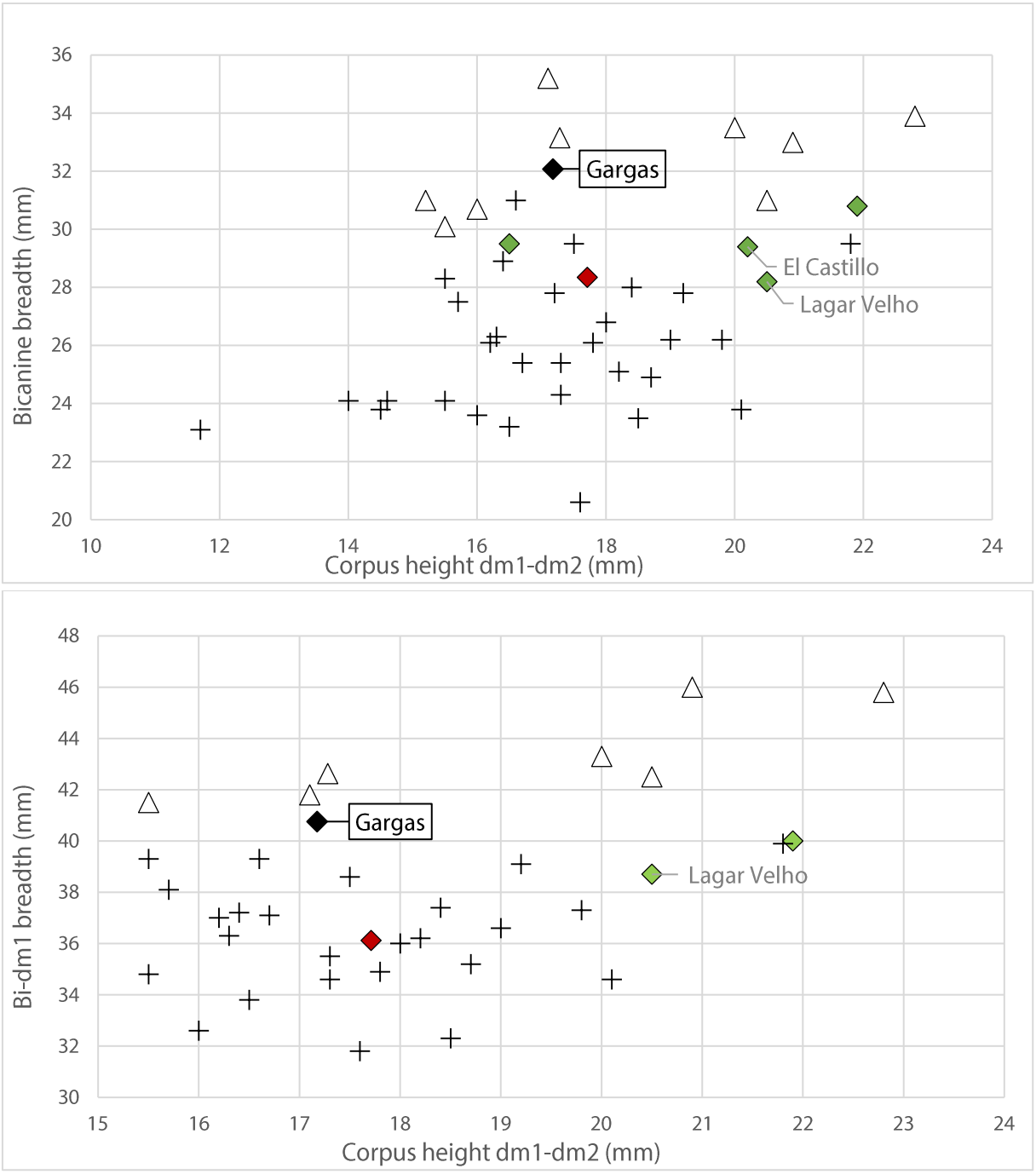

Figure S4. Bivariate plots of the bicanine breadth (top) and bi-dm1 breadth (bottom) against the corpus height of the Gargas mandible GPA-646 and the comparative specimens (triangles = Neandertal, green diamonds = Middle Upper Palaeolithic modern humans, red diamonds = Late Upper Palaeolithic modern humans, crosses = Holocene modern humans) / *Graphiques bivariés de la largeur bicanine (en haut) et de la largeur bi-dm1 (en bas) par rapport à la hauteur du corpus pour la mandibule de Gargas GPA-646 et les spécimens de comparaison (triangles = Néandertaliens, losanges verts = humains modernes du Paléolithique supérieur moyen, losanges rouges = humains modernes du Paléolithique supérieur final, croix = humains modernes de l'Holocène)*

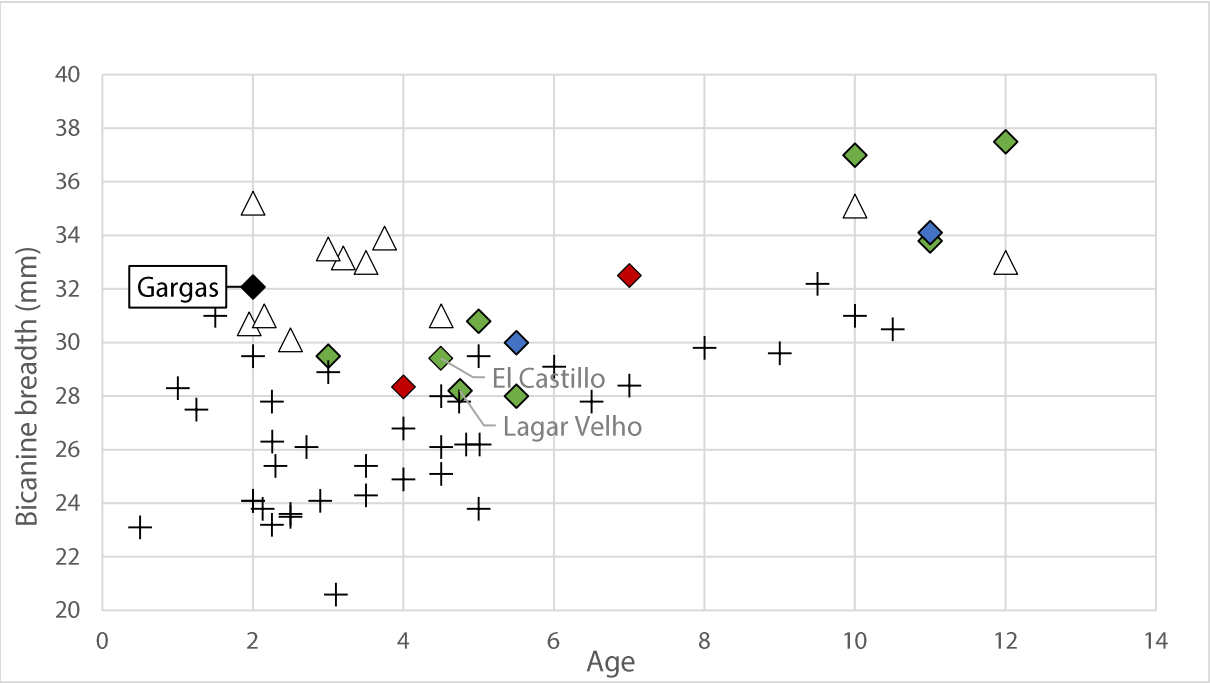

Figure S5. Bivariate plots of bicanine breadth against the age of the specimen for the Gargas mandible GPA-646 and comparative samples (triangles = Neandertal, blue diamonds = Early Palaeolithic modern humans, green diamonds = Middle Upper Palaeolithic modern humans, red diamonds = Late Upper Palaeolithic modern humans, crosses = Holocene modern humans) / *Graphiques bivariés de la largeur bicanine par rapport à l'âge du spécimen pour la mandibule de Gargas GPA-646 et les échantillons de comparaison (triangles = Néandertaliens, losanges bleus = humains modernes du Paléolithique supérieur ancien, losanges verts = humains modernes du Paléolithique supérieur moyen, losanges rouges = humains modernes du Paléolithique supérieur final, croix = humains modernes de l'Holocène)*

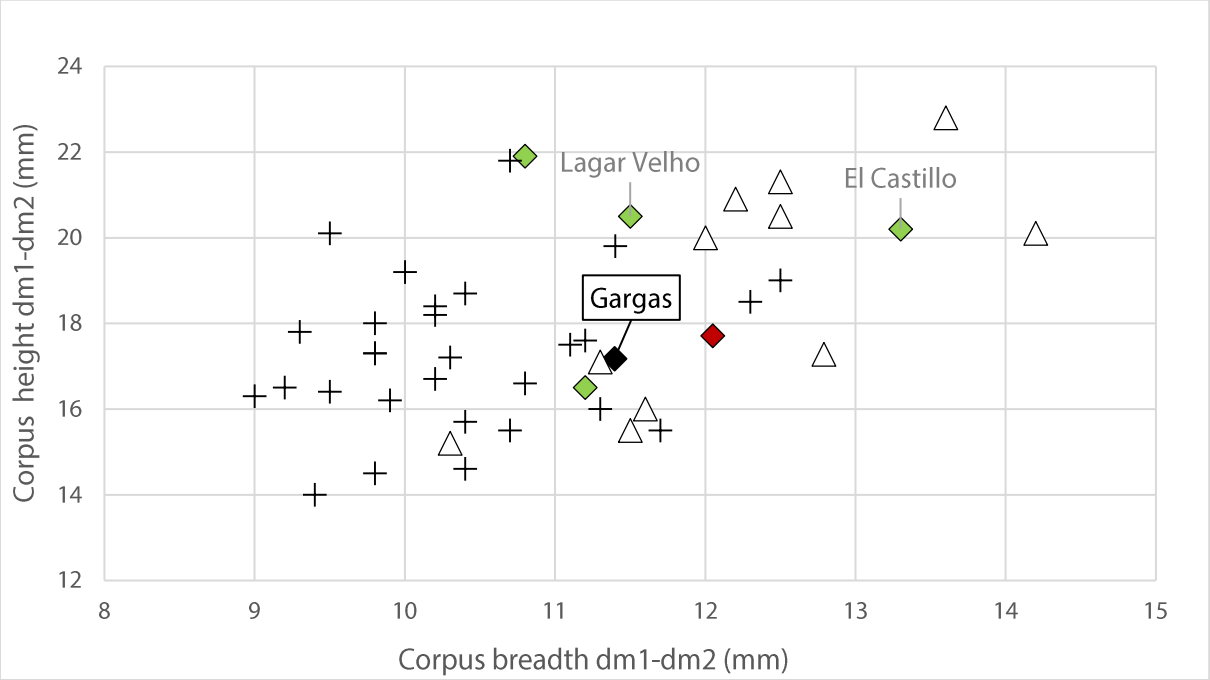

Figure S6. Bivariate plots of corpus height against the corpus breadth for the Gargas mandible GPA-646 and comparative specimens (triangles = Neandertal, green diamonds = Middle Upper Palaeolithic modern humans, red diamonds = Late Upper Palaeolithic modern humans, crosses = Holocene modern humans) / *Graphiques bivariés de la hauteur du corps par rapport à la largeur du corps pour la mandibule de Gargas GPA-646 et les échantillons de comparaison (triangles = Néandertaliens, losanges verts = humains modernes du Paléolithique supérieur moyen, losanges rouges = humains modernes du Paléolithique supérieur final, croix = humains modernes de l'Holocène)*

SI-7 Dental non-metric traits

Morphological traits were scored for the deciduous and permanent molars of GPA-646 (Table S10). The scoring of the cusp development for the deciduous molars is adapted from Hanihara (1961). All other traits are scored following the ASUDAS method (Turner et al. 1991) and its associated reference plaques, except for four traits (with asterisks) for which scores have been slightly modified by Le Luyer (2016). Definitions and scores of expressions for the non-metric traits analyzed in this study are recalled hereafter.

Table S10. Scores for 10 non-metric traits recorded on the LRdm1, the LLdm2, and the LLM1 of GPA-646. N/A: not applicable, NO: non-observable / *Valeurs obtenues pour les 10 traits non-métriques enregistrés sur la LRdm1, la LLdm2 et la LLM1 de GPA-646. N/A : non applicable, NO : non-observable*

Traits	**LRdm1**	**LLdm2**	**LLM1**
Hypoconulid	N/A	4	2
Entoconulid	N/A	0	0
Metaconulid	N/A	0	0
Protostylid	0	1	0
Groove pattern	N/A		1
Mid trigonid crest	N/A		0
Anterior fovea	1	0	0
Deflecting wrinkle	N/A		0
Cusp development	2	3	
Three-rooted lower molar	0	0	NO

Hypoconulid *(cusp 5)*: development of the cusp on the distobuccal aspect of the lower molars.
0-Absent: no occurrence of a hypoconulid.
1-Faint: the hypoconulid is very small.
2-Small: the hypoconulid is small.
3-Medium-sized: the hypoconulid is medium sized.
4-Large: the hypoconulid is large.
5-Very large: the hypoconulid is very large.

Entoconulid *(cusp 6, tuberculum sextum)*: development of the cusp on the distolingual aspect of the lower molars, lingually-placed from the hypoconulid.
0-Absent: the entoconulid is absent.
1-Faint: the entoconulid is much smaller than the hypoconulid.
2-Small: the entoconulid is smaller than the hypoconulid.
3-Medium-sized: the entoconulid is equal in size to the hypoconulid.
4-Large: the entoconulid is larger than the hypoconulid.
5-Very large: the entoconulid is much larger than the hypoconulid.

***Metaconulid** *(tuberculum intermedium, cusp 7)*: accessory cusp of the lower molars, between the metaconulid and the hypoconulid.
0-No occurrence of a metaconulid.
1-A faint tipless metaconulid occurs displaced as a bulge on the lingual surface.
2-A faint cusp is present.
3-The metaconulid is small.

4-The metaconulid is medium sized.
5-The metaconulid is large.

Protostylid: tubercule on the buccal surface of the lower molars.
0-No expression of any sort. Buccal surface is smooth.
1-A pit occurs in the buccal groove.
2-Curved groove: the buccal groove is curved distally.
3-Faint groove: a faint secondary groove extends mesially from the buccal groove.
4-Secondary groove is slightly more pronounced.
5-Secondary groove is stronger and can be easily seen.
6-Secondary groove extends across most of the buccal surface. This is considered a weak or small cusp.
7-A cusp with a free apex occurs.

***Groove pattern:** arrangement of the grooves and cusps on the lower molars.
0-A X-pattern is present, the protoconid and entoconid are in contact.
1-A Y-pattern is present, the metaconid and hypoconid are in contact.
2-The four main cusps are in contact.

***Mid trigonid crest:** a ridge that bridges the mesial aspects of the protoconid and the metaconid.
0-The crest is absent.
1-A crest connects the two cusps but it is interrupted by the central groove.
2-A continuous crest connects the two cusps.

Anterior fovea: expression of a fovea or groove on the anterior occlusal surface.
0-Absent: the anterior fovea is absent. The sulcus between the cusps continues without interruption from the center of the occlusal surface to the mesial border.
1-Faint groove: a weak ridge connects the mesial aspects of the protoconid and the metaconid producing a faint groove.
2-Small groove: the connecting ridge is larger and the resulting groove deeper than in grade 1.
3-Medium groove: the groove is longer than in grade 2.
4-Large groove: the groove is very long and mesial ridge is robust.

Deflecting wrinkle: form of variation of the medial ridge on the metaconid.
0-Deflecting wrinkle is absent. Medial ridge of the metaconid is straight.
1-Medial ridge of the metaconid is straight, but shows a midpoint constriction.
2-Medial ridge is deflected distally, but does not make contact with the entoconid.
3-Medial ridge id deflected distally forming an L-shaped ridge. The medial ridge contacts the entoconid.

Cusp development: number of cusps for the deciduous molars.
0-Presence of two cusps.
1-Presence of three cusps.
2-Presence of four cusps.
3-Presence of five cusps.
4-Presence of six cusps.

***Three-rooted lower molar**: presence of a third root for the lower molars.
0-Two roots: two separate roots exist for at least one-fourth of the total root length.

1-Three roots: a third (supernumerary) root is present on the distolingual aspect.
2-One root: a unique root in the form of a cone, root tip may be bifurcated, deep lingual and buccal developmental grooves can occur.

SI-8 Crown dimensions

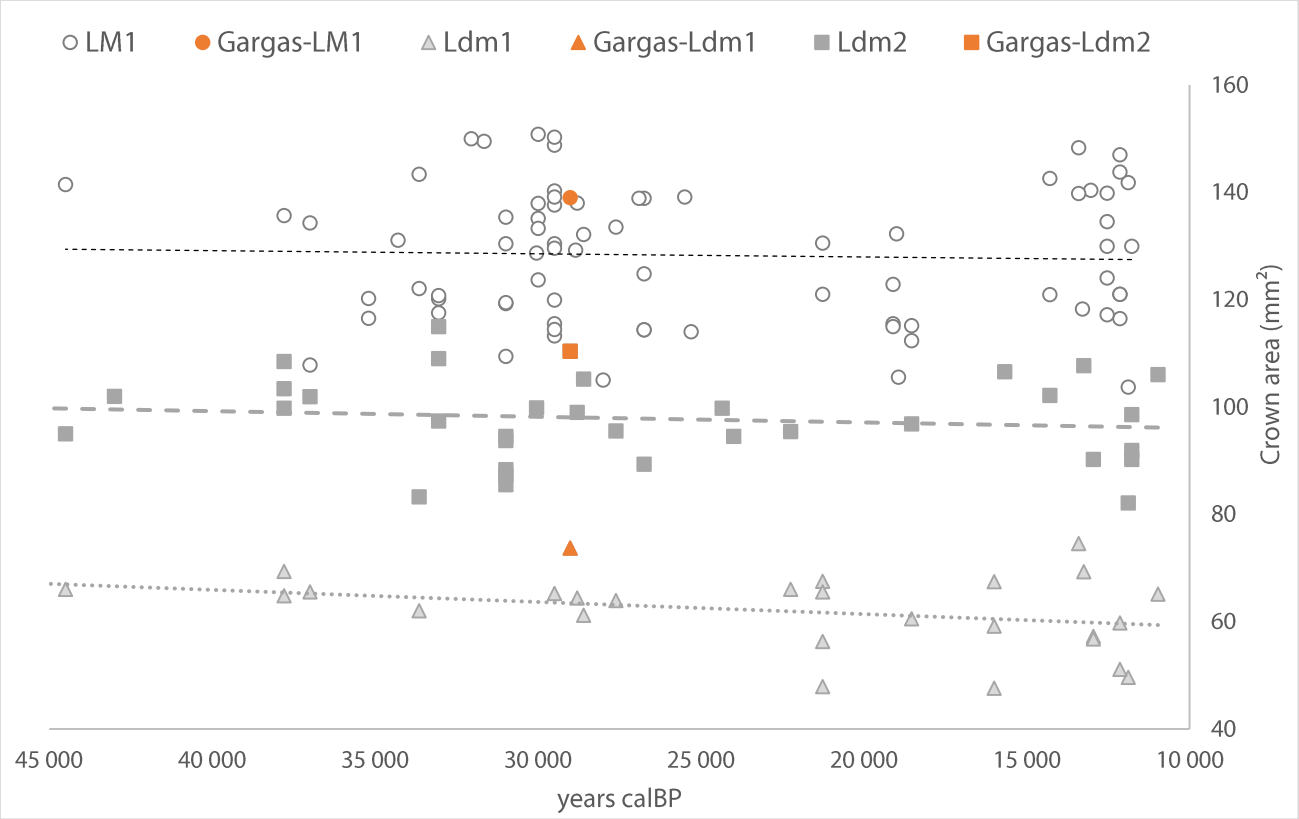

Figure S7. Crown area (BL*MD) for the Ldm1 (triangles), Ldm2 (squares) and LM1 (circles) of Gargas (in orange) and Upper Palaeolithic specimens (in grey) dated between *ca.* 45,000 and 10,000 cal BP / *Aire de la couronne (BL*MD) pour les Ldm1 (triangles), Ldm2 (carrés) et LM1 (cercles) de Gargas (en orange) et des spécimens du Paléolithique supérieur (en gris) datés entre ca. 45 000 et 10 000 cal BP*

Table S11. R Spearman's ranks correlation between mesiodistal (MD), buccolingual (BL), and crown area (MD*BL) dimensions, and latitude and longitude of the specimens / *Corrélation R de Spearman entre les dimensions mésiodistales (MD), buccolinguales (BL) et l'aire de la couronne (MD*BL), et la latitude et la longitude des spécimens*

Sample	Tooth	Variable	N	Latitude		Longitude	
				R Spearman	p value	R Spearman	p value
Entire Upper Palaeolithic sample	M1	MD	80	-0.04	0.757	0.02	0.858
		BL	98	-0.20	0.051	0.03	0.778
		Area	80	-0.17	0.141	0.07	0.532
	dm1	MD	33	-0.16	0.378	-0.13	0.454
		BL	41	-0.19	0.245	0.03	0.871
		Area	32	-0.23	0.212	-0.11	0.542
	dm2	MD	46	-0.24	0.113	**-0.49**	**0.001**
		BL	56	-0.21	0.129	**-0.36**	**0.006**
		Area	45	**-0.30**	**0.046**	**-0.52**	**<0.001**
45,000 - 20,000 year sample	M1	MD	54	-0.09	0.513	-0.03	0.842
		BL	59	-0.16	0.227	0.01	0.911
		Area	54	-0.16	0.238	0.02	0.867
	dm1	MD	21	-0.16	0.478	-0.03	0.892
		BL	21	-0.13	0.567	0.04	0.873
		Area	20	-0.26	0.278	-0.06	0.811
	dm2	MD	33	-0.32	0.068	**-0.45**	**0.009**
		BL	32	**-0.36**	**0.041**	**-0.39**	**0.028**
		Area	32	**-0.41**	**0.018**	**-0.53**	**0.002**
MUP sample only	M1	MD	38	0.06	0.707	0.02	0.918
		BL	42	-0.21	0.182	-0.35	0.022
		Area	38	-0.09	0.579	-0.07	0.668
	dm1	MD	9	0.03	0.931	0.05	0.897
		BL	8	-0.38	0.349	-0.29	0.490
		Area	8	-0.31	0.453	-0.26	0.528
	dm2	MD	18	**-0.51**	**0.030**	-0.44	0.068
		BL	17	-0.32	0.207	-0.15	0.567
		Area	17	**-0.50**	**0.039**	-0.43	0.085

Significant p-values are in bold.

SI-9 Dental tissue proportions and enamel thickness

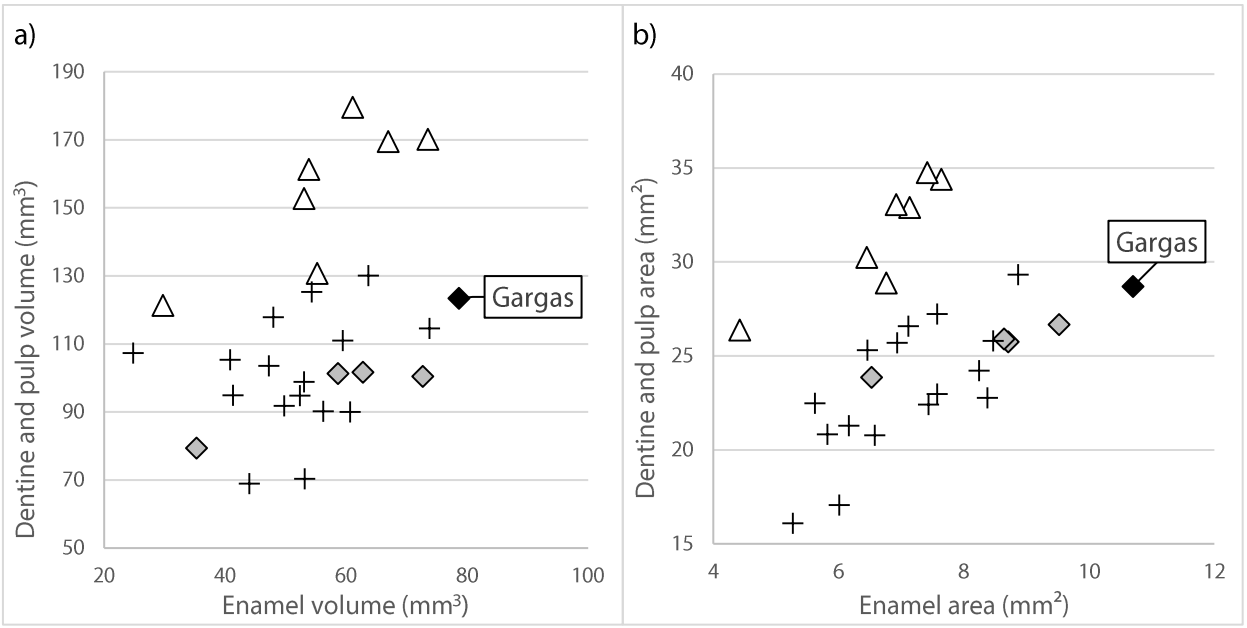

Figure S8. a) volumes and b) areas of enamel against the crown dentine and pulp for the LRdm1 of GPA-646 compared to those of Neandertals (triangles), Upper Palaeolithic (diamonds) and Holocene (crosses) modern humans / *a) volumes et b) aires de l'émail par rapport à la dentine et la pulpe dans la couronne pour la LRdm1 de GPA-646 comparés aux valeurs pour les individus Néandertaliens (triangles), du Paléolithique supérieur (losanges) et de l'Holocène (croix).*

SI-10 References

Aitken CG, Taroni F (2004) Statistics and the evaluation of evidence for forensic scientists. Wiley, Wiley Online Library, 450 p

Akazawa T, Muhesen S (2003) Neanderthal Burials - Excavations of the Dederiyeh Cave (Afrin, Syria). KW Publications, Auckland, 394 p

AlQahtani SJ, Hector MP, Liversidge HM (2010) Brief communication: The London atlas of human tooth development and eruption. American Journal of Physical Anthropology 142(3):481-490 [https://doi.org/10.1002/ajpa.21258]

Arsuaga JL, Gracia A, Martínez I et al (1989) The human remains from Cova Negra (Valencia, Spain) and their place in European Pleistocene human evolution. Journal of Human Evolution 18(1):55-92 [https://doi.org/10.1016/0047-2484(89)90023-7]

Arsuaga JL, Villaverde V, Quam R et al (2007) New Neandertal remains from Cova Negra (Valencia, Spain). Journal of Human Evolution 52(1):31-58 [https://doi.org/10.1016/j.jhevol.2006.07.011]

Bailey SE, Hublin J-J (2006) Dental remains from the Grotte du Renne at Arcy-sur-Cure (Yonne). Journal of Human Evolution 50(5):485-508 [https://doi.org/10.1016/j.jhevol.2005.11.008]

Bayle P (2008) Analyses quantitatives par imagerie à haute résolution des séquences de maturation dentaire et des proportions des tissus des dents déciduales chez les Néandertaliens et les Hommes modernes., Ph.D. thesis, Université de Toulouse III - Paul Sabatier, 344 p

Bayle P, Braga J, Mazurier A et al (2009a) Brief communication: high-resolution assessment of the dental developmental pattern and characterization of tooth tissue proportions in the late Upper Paleolithic child from La Madeleine, France. American Journal of Physical Anthropology 138(4):493-498 [https://doi.org/10.1002/ajpa.21000]

Bayle P, Braga J, Mazurier A et al (2009b) Dental developmental pattern of the Neanderthal child from Roc de Marsal: a high-resolution 3D analysis. Journal of Human Evolution 56(1):66-75 [https://doi.org/10.1016/j.jhevol.2008.09.002]

Bayle P, Le Luyer M, Robson Brown K (2017) The dental remains: enamel thickness, and tissue proportions In: Trinkaus E., Walker M. J. (eds) The people of Palomas: Neandertals from the Sima de las Palomas, Cabeza Gordo, Southeastern Spain. Texas A&M Press Anthropology Series, College Station, Texas, pp 115-137

Benazzi S, Viola B, Kullmer O et al (2011) A reassessment of the Neanderthal teeth from Taddeo cave (southern Italy). Journal of Human Evolution 61(4):377-387 [https://doi.org/10.1016/j.jhevol.2011.05.001]

Bergman CA, Stringer CB (1989) Fifty years after: Egbert, an early Upper Palaeolithic juvenile from Ksar Akil, Lebanon. Paléorient:99-111 [https://www.persee.fr/doc/paleo_0153-9345_1989_num_15_2_4512]

Billy G (1980) The Magdalenian child from the cave Le Figuier (Ardeche), France. Journal of Human Evolution 9:591-595 [https://doi.org/10.1016/0047-2484(80)90087-1]

Blanchard R, Peyrony D, Vallois H-V (1972) Le gisement et le squelette de Saint-Germain-la-Rivière. Masson, Paris, 115 p

Brabant H, Twiesselmann F (1964) Observations sur l'évolution de la denture permanente humaine en Europe occidentale. Bulletin du Groupement International pour la Recherche Scientifique en Stomatologie et Odontologie 7:11-84

Braga J, Heuzé Y (2007) Quantifying variation in human dental development sequences : an EVO-DEVO perspective In: Bailey S. E., Hublin J.-J. (eds) Dental perspectives on human evolution : state of the art research in dental anthropology. Springer, Berlin, pp 247-262

Bresson F (2000) Le squelette du Roc-de-Cave (Saint-Cirq-Madelon, Lot). PALEO 12(1): 29-59 [https://doi.org/10.3406/pal.2000.1595]

Bronk Ramsey C, Lee S (2013) Recent and planned developments of the program OxCal. Radiocarbon 55(2-3):720-730 [https://doi.org/10.1017/S0033822200057878]

Caillard P (1976) L'habitat nécropole de Téviec et les sépultures d'Hoëdic. Étude comparative de certaines dimensions dentaires et crâniennes. Bulletins et Mémoires de la Société d'Anthropologie de Paris 3(4):363-382 [https://doi.org/10.3406/bmsap.1976.1989]

Carretero JM, Quam RM, Gómez-Olivencia A et al (2015) The Magdalenian human remains from El Mirón Cave, Cantabria (Spain). Journal of Archaeological Science 60:10-27 [https://doi.org/10.1016/j.jas.2015.03.026]

Crevecoeur I (2008) Etude anthropologique du squelette du Paléolithique supérieur de Nazlet Khater 2 (Egypte). Apport à la compréhension de la variabilité passée des hommes modernes. Leuven University Press, Leuven, 318 p

De Lumley M-A (1973) Anténéandertaliens et néandertaliens du bassin méditerranéen occidental européen. Mémoire 2, Etudes quaternaires. Laboratoire de Paléontologie Humaine et Préhistoire, Université de Provence, 626 p

De Lumley M-A (1987) Les restes humains néandertaliens de la Brèche de Genay, Côte-d'Or, France. L'Anthropologie 91(1):119-162

de Lumley M-A, Giacobini G (2013a) Les néandertaliens de la Caverna delle Fate (Finale Ligure, Italie). I - Chronostratigraphie, restes squelettiques. L'Anthropologie 117(3):273-304 [https://doi.org/10.1016/j.anthro.2013.05.003]

de Lumley M-A, Giacobini G (2013b) Les néandertaliens de la Caverna delle Fate (Finale Ligure, Italie). II – Les dents. L'Anthropologie 117(3):305-344 [https://doi.org/10.1016/j.anthro.2013.05.002]

Dean M, Stringer C, Bromage T (1986) Age at death of the Neanderthal child from Devil's Tower, Gibraltar and the implications for studies of general growth and development in Neanderthals. American Journal of Physical Anthropology 70(3):301-309 [https://doi.org/10.1002/ajpa.1330700305]

Dean MC, Wood BA (2003) A digital radiographic atlas of great apes skull and dentition. In: Bondioli L., Macchiarelli R., editors. Digital archives of human paleobiology. Milan: ADS Solutions

Demirjian A, Goldstein H, Tanner JM (1973) A new system of dental age assessment. Human Biology 45(2):211-227 [https://www.jstor.org/stable/41459864]

Dobos A, Soficaru A, Trinkaus E (2010) The prehistory and paleontology of the Peştera Muierii, Romania. Etudes et recherches archéologiques de l'Université de Liège, Liège, 122 p

Duport L, Vandermeersch B (1976) La mandibule moustérienne de Montgaudier (Montbron, Charente). Comptes Rendus de l'Academie des Sciences de Paris 283(10):1161-1164

Fabbri PF (1987) Restes humains retrouvés dans la grotte Romanelli (Lecce, Italie) : Etude anthropologique. Bulletins et Mémoires de la Société d'Anthropologie de Paris 4(4):219-247 [https://doi.org/10.3406/bmsap.1987.1641]

Fabbri PF, Mallegni F (1988) Dental anthropology of the Upper Palaeolithic remains from Romito cave at Papasidero (Cosenza, Italy)/Anthropologie dentaire du Paléolithique supérieur, Grotte del Romito à Papasidero (Cosenza, Italie). Bulletins et Mémoires de la Société d'Anthropologie de Paris 5(3):163-177 [https://doi.org/10.3406/bmsap.1988.1671]

Faerman M, Zilberman U, Smith P et al (1994) A Neanderthal infant from the Barakai Cave, Western Caucasus. Journal of Human Evolution 27(5):405-415 [https://doi.org/10.1006/jhev.1994.1056]

Ferembach D (1957) Les restes humains de l'abri Lachaud. Bulletins et Mémoires de la Société d'Anthropologie de Paris 8(1-2):61-80 [https://doi.org/10.3406/bmsap.1957.2673]

Ferembach D (1969) Les affinités morphologiques de l'enfant néandertalien du Pech-de-l'Azé (Dordogne). Comptes Rendus de l'Academie des Sciences de Paris 268(D):1485-1488

Ferembach D, Legoux P, Fenart R et al (1970) L'enfant du Pech de l'Azé. Masson, Paris, 187 p

Formicola V (1986) Una mandibola umana dal deposito dell'Epigravettiano finale delle Arene Candide (scavi 1970). Rivista di Antropologia 64:271-278

Formicola V (1988) The triplex burial of Barma Grande (Grimaldi, Italy). HOMO - Journal of Comparative Human Biology 39:130-143

Foucher P, San Juan-Foucher C, Henry-Gambier D et al (2012) Découverte de la mandibule d'un jeune enfant dans un niveau gravettien de la grotte de Gargas (Hautes-Pyrénées, France) / Discovery of the

mandible of a young child in a Gravettian level of Gargas cave (Hautes-Pyrenees, France). PALEO 23:323-336 [https://doi.org/10.4000/paleo.2472]

Foucher P, San Juan-Foucher C, Villotte S et al (2019) Les vestiges humains gravettiens de la grotte de Gargas (Aventignan, France) : datations 14C AMS directes et contexte chrono-culturel. Bulletin de la Société Préhistorique Française 116(1):29-39

Frayer DW (1978) Evolution of the dentition in Upper Paleolithic and Mesolithic Europe. University of Kansas, Lawrence, 201 p

Frayer DW, Jelínek J, Oliva M et al (2006) Aurignacian male crania, jaws and teeth from the Mladeč caves, Moravia, Czech Republic. In: Teschler-Nicola M. (ed) Early Modern Humans at the Moravian Gate. Springer, Vienna, pp 185-272

Gambier D (1990-91) Les vestiges humains du gisement d'Isturitz (Pyrénées-Atlantiques). Etude anthropologique et analyse des traces d'action humaine intentionnelle. Antiquités nationales 22/23:9-26

Gambier D (1992) Vestiges humains du Paléolithique supérieur. Inventaire et description préliminaire de spécimens inédits des collections du Musée national de Préhistoire (Les Eyzies-de-Tayac). PALEO 4(1):91-100 [https://doi.org/10.3406/pal.1992.1196]

Gambier D (1994) Pont d'Ambon. Les vestiges humains. Gallia Préhistoire 36(1):108-112 [https://doi.org/10.3406/galip.1994.2101]

Gambier D, Houët F, Tillier A-M (1990) Dents de Font-de-Gaume (Chatelperronien et Aurignacien) et de La Ferrassie (Aurignacien ancien) en Dordogne. PALEO 2: 143-152 [https://doi.org/10.3406/pal.1990.994]

Gambier D, Lenoir M (1991) Les vestiges humains du Paléolithique supérieur en Gironde. Bulletin de la Société d'Anthropologie du Sud-Ouest XXVI(1):1-31

García Sánchez M (1987) Estudio preliminar de los restos neandertalenses del Boquete de Zafarrya (Alcaucín, Málaga) In: Arteaga O. (ed) Homenaje a Luis Siret (1934 a 1984) Actas del Congreso "Homenaje a Luis Siret" (1934–1984), Cuevas de Almanzora, Junio 1984. Dirección General de Bellas Artes de la Consejería de Cultura de la Junta de Andalucía, Madrid, pp 49-56

Garralda M-D, Maíllo-Fernández J-M, Higham T et al (2019) The Gravettian child mandible from El Castillo Cave (Puente Viesgo, Cantabria, Spain). American Journal of Physical Anthropology 170(3):331-350 [https://doi.org/10.1002/ajpa.23906]

Garralda M-D, Maureille B, Pautrat Y et al (2008) La molaire d'enfant néandertalien de Genay (Côte-d'Or, France). Réflexions sur la variabilité dentaire des Néandertaliens. PALEO 20:89-100 [https://doi.org/10.4000/paleo.1685]

Garralda M-D, Vandermeersch B (2000) Les Néandertaliens de la grotte de Combe-Grenal (Domme, Dordogne, France). PALEO 12:213-259 [https://doi.org/10.3406/pal.2000.1603]

Garralda MD, Tillier A-M, Vandermeersch B et al (1992) Restes humains de l'Aurignacien archaïque de la Cueva de El Castillo (Santander, Espagne). Anthropologie (Brno) 30(2):159-164

Genet-Varcin E, Miquel M (1967) Contribution à l'étude du squelette Magdalénien de l'abri Lafaye, à Bruniquel. L'Anthropologie 71(5-6):467-478

Gieseler W (1971) Germany. In: Oakley K. P., Campbell B. G., Molleson T. I. (eds) Catalogue of Fossil Hominids: Part II, Europe. British Museum, London

Glen E, Kaczanowski K (1982) Human Remains. In: Kozlowski J. K. (ed) Excavation of Bacho Kiro Cave (Bulgaria) Final Report. Panstwave Wydawnictwo Naukowe, Warszawa, pp 75-79

Gómez-Olivencia A, Crevecoeur I, Balzeau A (2015) La Ferrassie 8 Neandertal child reloaded: New remains and re-assessment of the original collection. Journal of Human Evolution 82:107-126 [https://doi.org/10.1016/j.jhevol.2015.02.008]

Gremyatskij MA (1949) The skull of the Neandertal child from the cave of Teshik-Tash, southern Uzbekistan (in Russian) In: Gremyatskij M. A., Nesturkh M. F. (eds) Teshik-Tash. Moscow State University, Moscow, pp 137-187

Gremyatskij MA, Nesturkh MF (1949) Teshik-Tash: Palaeolithic Man. Moscow State University, Moscow

Hanihara K (1961) Criteria for classification of crown characters of the human deciduous dentition. Journal of the Anthropological Society of Nippon 69:27-45 [https://doi.org/10.1537/ase1911.69.27]

Heim J-L (1982) Les enfants néandertaliens de La Ferrassie. Masson, Paris, 169 p

Heim J-L (1991) L'enfant magdalénien de la Madeleine. L'Anthropologie 95(2-3):611-638

Henry-Gambier D (2001) La sépulture des enfants de Grimaldi (Baoussé-Roussé, Italie) : anthropologie et palethnologie funéraire des populations dela fin du Paléolithique supérieur. Éditions du Comité des Travaux Historiques et Scientifiques, Paris, 177 p

Henry-Gambier D, Maureille B, White R (2004) Vestiges humains des niveaux de l'Aurignacien ancien du site de Brassempouy (Landes). Bulletins et Mémoires de la Société d'Anthropologie de Paris 16(1-2):49-87 [http://journals.openedition.org/bmsap/834]

Henry-Gambier D, Villotte S (2012) Les vestiges humains du Cuzoul-de-Vers : deux exemples de traitement du cadavre In: Clottes J., Giraud J.-P., Chalard P. (eds) Solutréen et Badegoulien au Cuzoul de Vers : Des chasseurs de rennes en Quercy. Etudes et Recherches archéologiques de l'Université de Liège, Liège, pp 367-385

Hillson SW (2006) Dental morphology, proportions, and attrition In: Trinkaus E., Svoboda J., Trinkaus E., Svoboda J. (eds) Early modern human evolution in Central Europe The people of Dolní Věstonice and Pavlov. Oxford University Press, New York, pp 179-223

Hrdlička A (1924) New data on the teeth of early man and certain fossil European apes. American Journal of Physical Anthropology 7(1):109-132 [https://doi.org/10.1002/ajpa.1330070117]

Kolosov IG, Kharitonov VM, Jakimov VP (1974) Discovery of the skeletal remains of a paleoanthrope at the Zaskalnaya VI site in the Crimea. Voprosy Antropol 46:79-88

Kolossov YG, Kharitonov VM, Yakimov VP (1975) Palaeoanthropic Specimens from the Site Zaskalnaya VI in the Crimea. De Gruyter Mouton, pp 419-428

Kondo O, Ishida H (2003) The Dentition of the Neanderthal Child of the Burial No. 2. In: Akazawa T., Muhesen S. (eds) Neanderthal Burials - Excavations of the Dederiyeh Cave (Afrin, Syria). KW Publications, Auckland, pp 323-335

Lacy S (2015) The dental metrics, morphology, and oral paleopathology of Oberkassel 1 and 2 In: Giemsch L., Schmitz R. W. (eds) The Late Glacial Burial from Oberkassel Revisited. Verlag Philipp von Zabern, Rheinische Ausgrabungen, pp 133-150

Le Luyer M (2016) Évolution dentaire dans les populations humaines de la fin du Pléistocène et du début de l'Holocène (19000 – 5500 cal. BP) : une approche intégrée des structures externe et interne des couronnes pour le Bassin aquitain et ses marges., Ph.D. thesis, Université de Bordeaux, 456 p

Le Roy M, Henry-Gambier D (2017) À propos des vestiges humains du Magdalénien du Sud-Ouest de la France : l'enfant inédit de l'abri Lafaye (Tarn et Garonne, France). PALEO 28:157-178 [https://doi.org/10.4000/paleo.3372]

Legoux P (1972) Étude odontologique des restes humains périgordiens et protomagdaléniens de l'Abri Pataud (Dordogne). Bulletins et Mémoires de la Société d'Anthropologie de Paris 9(4):293-330 [https://doi.org/10.3406/bmsap.1972.2055]

Legoux P (1974) Étude odontologique des restes humains périgordiens et proto-magdaléniens de l'Abri-Pataud (Dordogne) (seconde partie). Bulletins et Mémoires de la Société d'anthropologie de Paris, XIII° Série 1(1):45-84

Legoux P (1975) Présentation des dents des restes humains de l'Abri Pataud In: Movius Jr H. L. (ed) Excavation of the Abri Pataud Les Eyzies (Dordogne): Contributors. Peabody Museum, Harvard University, Cambridge, Massachusetts, pp 262-304

Leroi-Gourhan A (1958) Étude des restes humains fossiles provenant des Grottes d'Arcy-sur-Cure. Annales de Paléontologie 44:87-148

Madre-Dupouy M (1992) L'enfant du Roc de Marsal. Etude analytique et comparative. . Editions du CNRS, Paris, 299 p

Mallegni F (1995) The teeth and the periodontal apparatus of the Neandertal mandibles from the Guattari Cave (Monte Circeo, Lazio, Italy). Zeitschrift für Morphologie und Anthropologie 80(3):329-351 [http://www.jstor.org/stable/25757460]

Mallegni F, Naldini-Segre E (1992) A human maxilla (Fosselone 1) and scapula (Fosselone 2) recovered in the Pleistocene layers of the Fosselone Cave, Mt. Circeo, Italy. Quartenaria Nova II:211-225

Mallegni F, Palma di Cesnola A (1994) Sur quelques pièces gravettiennes de la Grotte Paglicci (Rignano Garganico, Pouilles, Italie). ANTHROPOLOGIE 32(1):45-57

Mallegni F, Parenti R (1972-1973) Studio antropologico di uno scheletro giovanile d'epoca gravettiana raccolto nella grotta Paglicci (Rignano Garganico). Rivista di Antropologia 58:317-348

Mallegni F, Ronchitelli A (1987) Découverte d'une mandibule néandertalienne à l'Abri du Molare près de Scario (Salerno - Italie) : observations stratigraphiques et paléthnologiques. Etude anthropologique. L'Anthropologie 91(1):163-174.

Mallegni F, Trinkaus E (1997a) A reconsideration of the Archi 1 Neandertal mandible. Journal of Human Evolution 33(6):651-668 [https://doi.org/10.1006/jhev.1997.0159]

Mallegni F, Trinkaus E (1997b) A reconsideration of the Archi 1 Neandertal mandible. Journal of Human Evolution 33(6):651-668 [https://doi.org/10.1006/jhev.1997.0159]

Manzi G, Passarello P (1995) At the Archaic/Modern Boundary of the Genus Homo: The Neandertals From Grotta Breuil. Current Anthropology 36(2):355-366 [https://doi.org/10.1086/204369]

Martin L (1985) Significance of enamel thickness in hominoid evolution. Nature 314:260-263 [https://doi.org/10.1038/314260a0]

Minellono F, Pardini E, Fornaciari G (1980) Le sepolture epigravettiane di Vado all' Arancio. Rivista di Scienze Preistoriche 35:6-44

Minugh-Purvis N (2000) Ontongeny and morphology of the child's mandible from Šipka - Moravia, Czech Republic. ANTHROPOLOGIE 38(1):71-82 [https://www.jstor.org/stable/26294843]

Mizoguchi Y (2002) Dental Remains Excavated at the Dederiyeh Cave during the 1989 to 1994 Seasons. In: Akazawa T., Muhesen S. (eds) Neanderthal Burials: Excavations of the Dederiyeh Cave, Afrin, Syria. International Research Center for Japanese Studies, Kyoto, pp 221-262

Olejniczak AJ, Smith TM, Feeney RN et al (2008) Dental tissue proportions and enamel thickness in Neandertal and modern human molars. Journal of Human Evolution 55(1):12-23 [https://doi.org/10.1016/j.jhevol.2007.11.004]

Palma di Cesnola A, Messeri P (1967) Quatre dents humaines paléolithiques trouvées dans des cavernes de l'Italie méridionale. Masson, Paris, 13 p

Pap I, Tillier A-M, Arensburg B et al (1996) The Subalyuk Neanderthal remains (Hungary): A re-examination. Annales historico-naturales musei nationalis hungarici 88:233-270

Patte É (1957) L'Enfant Néanderthalien du Pech de l'Azé. Masson, Paris, 230 p

Patte É (1968) L'homme et la femme de l'azilien de Saint-Rabier (fouilles Cheynier). Edition du Muséum, Paris, 56 p

Patte É (1976) Dents du Solutréen de Badegoule (fouilles Couchard). L'Anthropologie 80(1):65-74

Petit-Maire N, Ferembach D, Bouvier J-M et al (1971) France In: Oakley K. P., Campbell B. G., Molleson T. I. (eds) Catalogue of Fossil Hominids Part II : Europe. British Museum, London, pp 71-187

Pinilla B, Trinkaus E (2017) The Palomas dental remains: size and proportions In: Trinkaus E., Walker M. J. (eds) The people of Palomas: Neandertals from the Sima de las Palomas, Cabeza Gordo, Southeastern Spain. Texas A&M Press Anthropology Series, College Station, Texas, pp 89-104

Quam RM, Arsuaga J-L, Bermúdez de Castro J-Ma et al (2001) Human remains from Valdegoba Cave (Huérmeces, Burgos, Spain). Journal of Human Evolution 41(5):385-435 [https://doi.org/10.1006/jhev.2001.0486]

Rak Y, Kimbel WH, Hovers E (1994) A Neandertal infant from Amud Cave, Israel. Journal of Human Evolution 26(4):313-324 [https://doi.org/10.1006/jhev.1994.1019]

Reimer PJ, Bard E, Bayliss A et al (2013) IntCal13 and marine13 radiocarbon age calibration curves 0-50,000 years cal BP. Radiocarbon 55(4):1869-1887 [https://doi.org/10.2458/azu_js_rc.55.16947]

Sakura H (1970) State of the skeleton of the Amud Man in situ. In: Suzuki H., Takai F. (eds) THe Amud Man and His Cave Site. Tokyo University Press, Tokyo, pp 117-122

Sergi S, Parenti R, Paoli G (1974) Il giovane paleolitico della Caverna delle Arene Candide. Memorie dell'Istituto di Paleologia Umana 2:13-38

Sladek V, Trinkaus E, Hillson S et al (2000) The People of the Pavlovian: Skeletal Catalogue and Osteometrics of the Gravettian Fossil Hominids from Dolní Věstonice and Pavlov. Academy of Sciences of the Czech Republic, Institute of Archaeology, Brno, 244 p

Smith BH (1984) Patterns of molar wear in hunter–gatherers and agriculturalists. American Journal of Physical Anthropology 63(1):39-56 [https://doi.org/10.1002/ajpa.1330630107]

Smith TM, Olejniczak AJ, Zermeno JP et al (2012) Variation in enamel thickness within the genus *Homo*. Journal of Human Evolution 62(3):395-411 [https://doi.org/10.1016/j.jhevol.2011.12.004]

Teschler-Nicola ME, Antl-Weiser W, Prossinger H (2004) Two Gravettian human deciduous teeth from Grub/Kranawetberg, Lower Austria. HOMO - Journal of Comparative Human Biology 54(3):229-239 [https://doi.org/10.1078/0018-442X-00074]

Tillier A-M (1979a) La dentition de l'enfant moustérien Chateauneuf 2 découvert à Hauteroche (Charente). L'Anthropologie 83(3):417-438 [https://halshs.archives-ouvertes.fr/halshs-00454468]

Tillier A-M (1979b) Restes crâniens de l'enfant moustérien homo 4 de Qafzeh (Israël), la mandibule et les maxillaires. Paléorient:67-85 [https://doi.org/10.3406/paleo.1979.4240]

Tillier A-m (1982) Les enfants néanderthaliens de Devil's Tower (Gibraltar). Zeitschrift für Morphologie und Anthropologie 73(2):125-148 [https://www.jstor.org/stable/25756601]

Tillier A-M (1983) Le crâne d'enfant d'Engis 2 : un exemple de distribution des caractères juvéniles, primitifs et néanderthaliens. Bulletin de la Société royale belge d'Anthropologie et de Préhistoire 94:51-75 [https://biblio.naturalsciences.be/associated_publications/anthropologica-prehistorica/bulletin-de-la-societe-royale-belge-d-anthropologie-et-de-prehistoire/ap-094-1983/ap94_51-75.pdf]

Tillier A-M, Arensburg B, Vandermeersch B et al (2003) New human remains from Kebara Cave (Mount Carmel). The place of the Kebara hominids in the Levantine Mousterian fossil record. Paléorient:35-62 [https://doi.org/10.3406/paleo.2003.4764]

Tillier AM, Genet-Varcin E (1980) La plus ancienne mandibule d'enfant découverte en France dans le gisement de La Chaise de Vouthon (Abri Suard) en Charente. Zeitschrift für Morphologie und Anthropologie 71(2):196-214 [https://www.jstor.org/stable/25756479]

Trinkaus E (1976) Note on the hominid molar from the Abri des Merveilles at Castel-Merle (Dordogne). Journal of Human Evolution 5(2):203-205 [https://doi.org/10.1016/0047-2484(76)90021-X]

Trinkaus E (1983) The Shanidar Neandertals. Academic Press, New York, 502 p

Trinkaus E (2018) An abundance of developmental anomalies and abnormalities in Pleistocene people. Proceedings of the National Academy of Sciences 115(47):11941-11946 [https://doi.org/10.1073/pnas.1814989115]

Trinkaus E, Bailey S, Zilhão J (2001) Upper Paleolithic human remains from the Gruta do Caldeirão, Tomar, Portugal. Revista Portuguesa de Arqueologia 4(2):5-17

Trinkaus E, Bailey SE, Davis SJMZ, J. (2011) The Magdalenian human remains from the Galera da Cisterna (Almonda karstic system, Torres Novas, Portugal) and their archeological context. Arqueologo Portugues 5(1):395-413

Trinkaus E, Buzhilova AP, Mednikova MB et al (2014) The People of Sunghir: Burials, Bodies and Behavior in the Earlier Upper Paleolithic. Oxford University Press, New York, 339 p

Trinkaus E, Hillson SW, Franciscus RG et al (2006) Skeletal and dental paleopathology In: Trinkaus E., Svoboda J., Trinkaus E., Svoboda J. (eds) Early modern human evolution in Central Europe The people of Dolní Věstonice and PavlovNew York, pp 419-458

Trinkaus E, Moldovan O, Milota ş et al (2003) An early modern human from the Peştera cu Oase, Romania. Proceedings of the National Academy of Sciences 100(20):11231-11236 [https://doi.org/10.1073/pnas.2035108100]

Trinkaus E, Svoboda J (2006) Early modern human evolution in Central Europe : the people of Dolní Věstonice and Pavlov. Oxford University Press, Oxford, 500 p

Turner CG, Nichol CR, Scott GR (1991) Scoring procedures for key morphological traits of the permanent dentition: the Arizona State University Dental Anthropology System In: Kelly M., Larsen C. S. (eds) Advances in Dental Anthropology. Wiley-Liss, Inc., New-York, pp 13-31

Vallois H-V (1972) Le crâne magdalénien des Hoteaux: notes anthropologiques. Bulletins et Mémoires de la Société d'Anthropologie de Paris 12(9):7-25 [https://doi.org/10.3406/bmsap.1972.2037]

Vallois H-V, de Felice S (1977) Les Mésolithiques de France : étude anthropologique. Masson, Paris, 194 p

Vandermeersch B (1984) A propos de la découverte du squelette néandertalien de Saint-Césaire. Bulletins et Mémoires de la Société d'Anthropologie de Paris 1(XIV):191-196 [https://doi.org/10.3406/bmsap.1984.3932]

Verdène J (1975) La denture des hommes du Paléolithique supérieur et du Mésolithique français, Ph.D. thesis, Université de Paris VII, 317 p

Verna C (2006) Les restes humains moustériens de la Station Amont de la Quina - (Charente, France) : contexte archéologiqe et constitution de l'assemblage : étude morphologique et métrique des restes crânio-faciaux : apport à l'étude de la variation néandertalienne, Ph.D. thesis, Université de Bordeaux 1, 629 p

Verna C, Dujardin V, Trinkaus E (2012) The Early Aurignacian human remains from La Quina-Aval (France). Journal of Human Evolution 62(5):605-617 [https://doi.org/10.1016/j.jhevol.2012.02.001]

Vieland VJ (1998) Bayesian Linkage Analysis, or: How I Learned to Stop Worrying and Love the Posterior Probability of Linkage. American Journal of Human Genetics 63:947-954 [https://doi.org/10.1086/302076]

Villotte S, Chiotti L, Nespoulet R et al (2015) Étude anthropologique des vestiges humains récemment découverts issus de la couche 2 de l'abri Pataud (Les Eyzies-de-Tayac-Sireuil, Dordogne, France). Bulletins et Mémoires de la Société d'Anthropologie de Paris 27:158-188 [https://doi.org/10.1007/s13219-015-0128-3]

Villotte S, Ogden AR, Trinkaus E (2018) Dental Abnormalities and Oral Pathology of the Pataud 1 Upper Paleolithic Human. Bulletins et Mémoires de la Société d'Anthropologie de Paris 30(3-4):153-161

Villotte S, Samsel M, Sparacello V (2017) The paleobiology of two adult skeletons from Baousso da Torre (Bausu da Ture) (Liguria, Italy): Implications for Gravettian lifestyle. Comptes Rendus Palévol 16(4):462-473 [https://doi.org/10.1016/j.crpv.2016.09.004]

Vlček E (1969) Neandertaler der Tschechoslowakei. Tschechoslowakische Akademie der Wissenschaften, Prag, 276 p

Voisin J-L, Condemi S, Wolpoff MH et al (2012) A new online database (http://anthropologicaldata.free.fr) and a short reflection about the productive use of compiling internet data. PaleoAnthropology 2012:241-244 [https://doi.org/10.4207/PA.2012.ART76]

Walker MJ, Lombardi AV, Zapata J et al (2010) Neandertal mandibles from the Sima de las Palomas del Cabezo Gordo, Murcia, southeastern Spain. American Journal of Physical Anthropology 142(2):261-272 [https://doi.org/10.1002/ajpa.21223]

Weinert H (1925) Der Schädel des eiszeitlichen Menschen von Le Moustier in neuer Zusammensetzung. Springer, Berlin

Zilhão J, Trinkaus E (2002) Portrait of the artist as a child. The Gravettian human skeleton from the Abrigo do Lagar Velho and its archeological context, 1st. ed edn. Instituto Português de Arqueologia, Lisboa, 609 p